Micro-trabeculae, macro-plaques or mini-basement membranes in human term fetal membranes?

COLIN OCKLEFORD, NICHOLAS BRIGHT, ANDREW HUBBARD, CHRISTOPHER D'LACEY, JAMES SMITH, LISA GARDINER, TANYA SHEIKH, MELISSA ALBENTOSA AND KATE TURTLE

Advanced Light Microscope Facility, Department of Anatomy, University of Leicester Medical School, University Road, Leicester LE1 9HN, U.K.

[Plate 1]

SUMMARY

Immunocytochemical confocal laser scanning microscopy and ultrastructural analysis, including immunoelectron microscopy, reveals the distribution of structures in human term amniochorion similar in some respects to basement membranes but with unusually restricted dimensions. On the basis of their immunoreactivity, these trabecular structures, found on the fibroblast layer side of the spongy layer of human term amniochorion and adjacent reticular layer, have been shown to contain type IV collagen, laminin, and nidogen. The origin of these components may be from primitive epithelial structures which pumped fluid into the lakes that eventually coalesced to form the extraembryonic coelom separating the extraembryonic somatic mesoderm from the extraembryonic splanchnic mesoderm. Such a theory of their origin might link them with the mysterious 'cellular layer', a single-cell-thick layer of cells which is usually no longer present in fetal membranes at term. The similarity in composition but not in size of these structures to anchoring plaques for type VII collagen is possible support for the view that these structures are integrators of extracellular matrix polymeric proteins.

The 'pseudobasement' membrane associated with the trophoblast layer, on investigation, appears to be typical by six criteria.

'Coiled' fibrous structures in the extracellular matrix of the spongy layer may aid adjustments under tension at this shear surface by a detachable 'Velcro' or 'two spring' fastening system. The coils are rich in fibronectin.

The suggestion is made that the compact layer is a giant lamina reticularis associated with the amniotic epithelial basement membrane.

1. INTRODUCTION

The conventional view of type IV collagen is that it is a molecular form restricted in its distribution to basal laminae (Sage 1982; Modesti *et al.* 1989). Recent evidence, however, shows that smaller amounts of these molecules also exist in sites distant from the basal laminae (Pratt & Madri 1985; Nanaev *et al.* 1991).

We have observed type IV collagen and associated molecules with epifluorescence light microscopy and immunoelectron microscopy. The protein is distributed classically in near-continuous form in the basement membrane underlying the amniotic epithelium (Malak *et al.* 1993). Type IV collagen is also found in the 'pseudobasement' membrane (Malak *et al.* 1993). This latter structure (Bourne 1962, 1966) is closely associated with the basal layer of cytotrophoblast cells of the chorion laeve. It is slightly thinner than the amniotic epithelial basement membrane but is also continuous. Thus there is a basement membrane for both the chorionic and the amniotic epithelium. The third type IV collagen-containing component of the tissue, the spongy layer, is thought to be a remnant of the extraembryonic coelom which becomes trapped between the chorion and the expanding amnion. In the immediately adjacent fibroblast layer the type IV collagen-containing structures we call micro-trabeculae are described here for the first time.

2. MATERIALS AND METHODS

(*a*) *Tissue sampling*

Material was obtained from human fetal membranes obtained immediately after the live births of 15 healthy babies following normal delivery at the Maternity Hospital of Leicester Royal Infirmary.

Tissue was cut into strips and rolled with the amnion innermost before immersion in OCT (BDH) cryo-embedding medium. The roll was held vertical and the container was frozen at −70°C in a CO_2-hexane slush. Material was stored at −40°C before sectioning.

(*b*) *Cryosectioning*

Sections 5–10 μm thick were cut by using a Leitz

cryostat. They were melted onto glass slides and used either unfixed or fixed in 3% formaldehyde, washed twice in phosphate buffered saline (PBS) at pH 7.3, treated for 10 min in 0.05% Triton × 100 and then further washed in PBS until the surface tension returned to the glass slide.

(*c*) *Indirect immunofluorescence technique*

Indirect immunofluorescence preparations were made as previously described (Bradbury & Ockleford 1990; Ockleford 1990).

Primary antibodies used were: (i) a mouse IgG1 anti-laminin (purified human) monoclonal antibody obtained from Sigma Immunochemicals (Code No. L8271; Lot 50H4807) was used in the range of dilutions 1/10 to 1/100; (ii) a mouse monoclonal IgG1 anti-type IV collagen (from human kidney) antibody obtained from Dako (Code No M785) was used at 1/100 dilution; (iii) a rabbit polyclonal anti-type IV collagen antibody obtained from Sanbio; (iv) a rabbit polyclonal anti-nidogen antiserum (1001) was raised by R.Timpl against recombinant mouse basement membrane proteins; and (v) a mouse monoclonal anti-human fibronectin (clone FN-15; lot 49F4806) was used in the form of ascites obtained from Sigma (St. Louis).

Second step antibody conjugates were: (i) fluorescein isothiocyanate conjugated rabbit anti-mouse antibody, code no. 65–171–3 (ICN Biochemicals); (ii) fluorescein isothiocyanate conjugated Goat anti-rabbit IgG (Monosan Antibodies, Sanbio b.v. Biological Products); (iii) Texas red conjugated Goat anti-rabbit IgG (Monosan Antibodies, Sanbio b.v. Biological Products). Non-immune sera for blocking and control experiments were obtained from Sigma Immunochemicals Ltd, as follows: mouse, code number M5905; goat, code number G9023; rabbit, code number R9133.

(*d*) *Dual labelling*

(*i*) *Collagen IV and laminin*

Dual labelling was done by applying first the monoclonal anti-laminin antibody (1/100 dilution) raised in mouse and then the rabbit polyclonal anti-type IV collagen antibody (1/10). The former was identified by using a 1/50 dilution of sheep anti-mouse FITC conjugate. Following this, a goat anti-rabbit Texas red conjugate was used (dilution 1/150) to identify the anti-type IV collagen antibody.

(*ii*) *Fibronectin and laminin*

The anti-laminin immunofluorescence was done as indicated above but after application of rabbit anti-fibronectin at 1/100 dilution. The anti-fibronectin second step was a 1/150 dilution of goat-anti rabbit Texas Red.

(*e*) *Fluorescence microscopy*

Immunolabelled frozen sections were mounted in photobleach retardant mountant (Citifluor; Platt & Michael 1983).

A Zeiss standard epifluorescence microscope was used to evaluate preparations. More detailed microscopy was done by using a Biorad Lasersharp M.R.C. 600 confocal system mounted on a Zeiss axiovert equipped with infinity corrected optics. These methods have been described in detail earlier (Ockleford *et al.* 1981; Bradbury & Ockleford 1990).

(*f*) *Immunoelectron microscopy and low-temperature embedding*

Tissue was fixed within 2 min of removal by Caesarian Section either in 3% formaldehyde in 0.1 M PBS or in 0.1% glutaraldehyde plus 3% formaldehyde in 0.1 M PBS. Both fixatives were buffered to pH 7.4 and contained 0.5 mM $CaCl_2$ additive. Fixation was for 2 h at room temperature. Aldehyde was quenched by using 50 mM NH_4Cl in PBS for 30 min at 4°C. Tissue was washed in PBS (3 × 20 min and overnight at 4°C). Dehydration was effected in 1 h steps in an ethanol series as follows: 50%, −20°C; 70%, −42°C; 90%, −42°C; 100%, −70°C; 100%, −70°C. Infiltration and embedding was done by using HM23 resin (Lowi GmbH) as follows. Resin:ethanol mixture steps; 1:1, −70°C, 1 h; 2:1, −70°C, 1 h; pure resin, −70°C, 1 h; pure resin, −70°C, overnight; pure resin, −70°C, 8 h. The progressive lowering of temperature was accomplished by using a high thermal conductivity aluminium block designed to minimize temperature gradients in the solutions used to dehydrate and embed the tissue. Each subsequent solution was pre-cooled and drawn through from a second chamber in the block. Finally, the tissue was transferred to fresh, pre-cooled resin in gelatin capsules and cured in an aluminium UV polymerization chamber using 360 nm irradiation at −23°C for 24 h. Blocks were stored at room temperature.

Ultrathin sections were cut by using a Reichart OMU-4 ultramicrotome and mounted on 300 mesh Ni grids (Gilder). Amidination of free aldehyde was with 50 mM NH_4Cl in PBS for 10 min at room temperature.

Blocking of non-specific binding was done by using 1% bovine serum albumin, 5% non-immune goat serum in PBS for 10 min at room temperature. First step incubation was with 1/50 dilution of Dako mouse monoclonal antibody against human collagen IV (Dako) plus blocking reagents at 4°C overnight. The first step antibody was replaced by a 1/50 dilution of non-immune mouse IgG in control experiments. Washing was done for a total of 20 min in several changes of PBS solution. Second step antibody (1/100 dilution of biotinylated goat anti-mouse IgG, Amersham) was applied by using the PBS plus blocking reagents as a vehicle for 1 h at 37°C. The previous washing protocol was repeated, and the sections were then reacted with a 1/100 dilution of Extravidin (Sigma) adsorbed to monodisperse 10 nm gold colloid particles at 37°C for 1 h.

Grids were washed for 2 × 2 min in 1% BSA in PBS

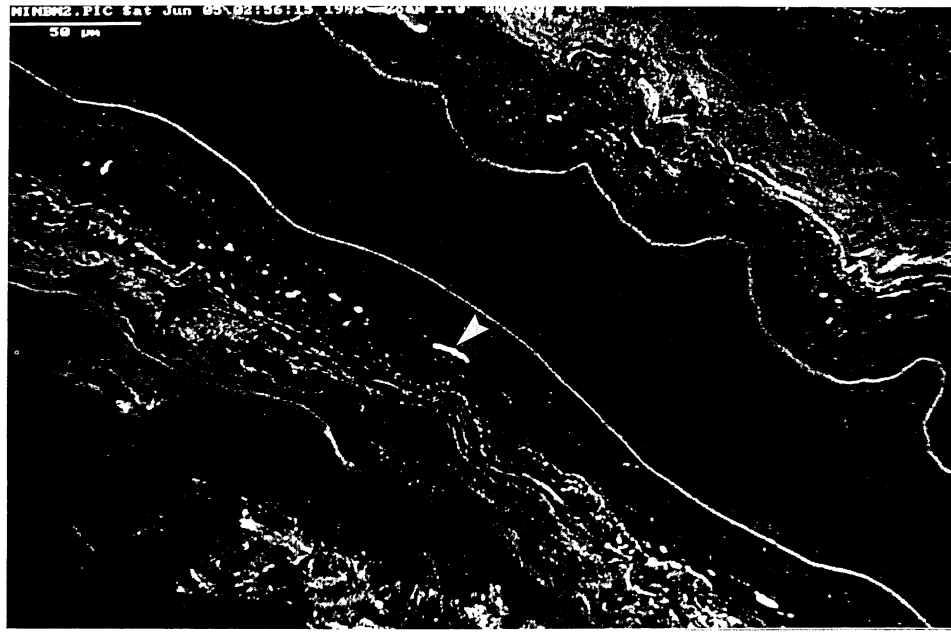

Figure 1. Confocal indirect immunofluorescence micrograph showing the distribution of anti-type IV collagen immunoreactivity. The tissue is folded with the amniotic layers facing inwards along the diagonal from top left to bottom right. The continuous lines of the two amniotic epithelial basement membranes are shown. A series of trabeculae are visible in the fibroblast layer. A particularly large one of these is arrowed.Scale bar denotes 50 μm.

followed by 3 × 2 min in PBS alone followed by 3 × 2 min in filtered distilled water. Grids were finally rinsed in acetone. Gold-labelled sections were counterstained by using 2% aqueous uranyl acetate. Grids were viewed by using a Jeol 100-CX electron microscope operated at an accelerating voltage of 80 kV.

3. RESULTS

(*a*) *Type IV collagen*

The immunofluorescence technique confirmed the previously described distribution of type IV collagen (Malak *et al.* 1993). The results found with both of the anti-type IV collagen antibodies were indistinguishable. Relatively intense fluorescence was associated with the amniotic epithelial basement membrane (figures 1 and 3*a*) and the chorion laeve (pseudobasement) membrane (figure 5). The extracellular space of the trophoblast layer was consistently reactive, as was that of the reticular layer (figure 1). Some immunoreactivity was detected in the decidual extracellular matrix. This was particularly pronounced surrounding the small blood vessels in that tissue where it was coincident in Nomarski images with the basal lamina of the endothelial cells forming the blood vessel walls.

It was possible in a number of preparations to observe structures showing immunoreactivity with anti- type IV collagen antibodies which have not been described previously in this situation (figures 1 and 2*a–c*). These take the form of trabeculae on average 7.6 μm in length ($n = 127$, s.d. = 2.54). They are of varying width, the mean being 1.4 μm ($n = 129$, s.d. = 0.61). They are seen in groups with rather irregular spacing. The orientation of these structures usually occurs with the longer axis parallel to the tissue planes; however, they are also sometimes disoriented, even being found orthogonal to the layers of the tissues in the section (figures 1 and 2).

Table 1 shows mean dimensional and fluorescence intensity measurements of various collagen IV containing structures in 24 picture files of frozen sections through amniochorion reacted in an indirect immunofluorescence protocol and imaged by using the confocal laser scanning microscope. The amniotic epithelium basement membrane has a mean width of 1.8 μm ($n = 137$, s.d. = 1.39). The basement membrane of the chorion laeve trophoblast (pseudobasement membrane) has a mean width of 1.9 μm ($n = 44$, s.d. = 0.61). 'Coil-like' structures which are immunoreactive in the region of the spongy layer (figures 3*a,b* and 4*a,b*) have an overall mean width of 10.9 μm ($n = 92$, s.d. = 2.00), whereas the fibres that comprise the coil-like structures have a mean width of 1.1 μm ($n = 87$, s.d. = 0.40). The trabecular structures in the fibroblast layer exhibited a mean immunofluorescence intensity (217.90) not significantly different (at the 1% level) from that of the amniotic basement membrane (222.68) and chorion laeve basement membrane (213.50). These structures share the highest levels of immunofluorescence in the tissue.

One point of note in several indirect immunofluorescence preparations using the anti-type IV collagen antibodies was the presence of a narrow zone of reduced fluorescence intensity on the reticular layer side of the chorion laeve basement membrane. This was crossed at intervals by strands of anti-type IV collagen reactive matrix (figure 5).

Analysis of variance showed that the mean length of the spongy layer fibres (11.7 μm) was significantly

Figure 2. For description see opposite.

Table 1. *Linear and fluorescence intensity (grey scale) measurements made from different areas of the sections through the term membranes studied; measurements were made using SOM and COMOS (Biorad) software*

(*a*)

	width of structure (μm)				
	amniotic basement membrane	fibroblast layer microtrabeculae	spongy layer fibres	spongy layer coils	trophoblast basement membrane
mean	1.8	1.4	1.1	10.9	1.9
sample s.d.	1.4	0.6	0.4	2.0	0.6
sample variance	1.9	0.4	0.2	3.9	0.4
number of samples	137	129	87	92	44

(*b*)

	length of structure (μm)				
	amniotic basement membrane[a]	fibroblast layer microtrabeculae	spongy layer fibres	spongy layer coils[a]	trophoblast basement membrane[a]
mean	—	7.6	11.7	—	—
sample s.d.	—	2.5	4.0	—	—
sample variance	—	6.4	16.4	—	—
number of samples	—	127	88	—	—

(*c*)

	immunofluorescence intensity of structure (0–255)				
	amniotic basement membrane	fibroblast layer microtrabeculae	spongy layer fibres	spongy layer coils[b]	trophoblast basement membrane
mean	222.68	217.90	169.47	—	213.50
sample s.d.	17.89	20.96	44.54	—	23.90
sample variance	319.91	439.40	1983.88	—	571.68
number of samples	60	60	60	—	60

[a] Length measurements were not made of structures extending beyond the microscope field.
[b] Intensity readings were not taken from these heterogeneous structures.

longer than the mean length (7.6 μm) of the fibroblast layer microtrabeculae ($F=84.2$, $p \ll 0.01$). A significant difference was also found between the mean width of the spongy layer coil (10.9 μm) and mean widths of the other four structures. The mean width of the chorion laeve basement membrane (1.9 μm) was also significantly larger than the mean width of the spongy layer fibre (1.1 μm) and the mean width of the fibroblast layer microtrabeculae (1.4 μm). The mean width of the spongy layer fibre was also significantly smaller than the mean width (1.8 μm) of the amniotic basement membrane ($F=43.7$, $p<0.01$). On a scale of 0 to 255, the mean intensity of the spongy layer fibres (169.47) was significantly lower than the mean intensities of the amniotic basement membrane (222.68), the fibroblast layer microtrabeculae (217.90) and the chorion laeve basement membrane (213.50) ($F=43.7$, $p \ll 0.01$).

No correlation was sought between dimensional and intensity measurements of structures because two independent data sets were obtained suited to the particular measurements made. The lengths of the spongy layer fibres significantly correlated with the widths of the amniotic epithelial basement membrane ($r=0.4208$, $p<0.01$) and also the fibroblast layer microtrabeculae ($r=0.4517$, $p<0.01$). The fibroblast layer microtrabeculae widths also correlated with the spongy layer fibre widths ($r=0.3116$, $p<0.05$). The intensity of the chorion laeve basement membrane corrrelated with the spongy layer fibre intensity ($r=0.4248$, $p<0.01$) but not with other measures.

Ultrastructural immunocytochemistry using low denaturation embedding protocols preserves the ultrastructural morphology of the basal laminae and its anti-type IV collagen immunoreactivity (figures 9, 10, 11 and 12). Thus colloidal gold labelling is concen-

Figure 2. A series of high-resolution confocal indirect immunofluorescence micrographs showing the immunoreactivity of trabeculae to anti-type IV collagen. The images are projections of extended focus series reconstructed from a stack of over 30 optical sections (see overlays). In (*c*) the amniotic epithelial basement membrane (asterisk) and the edge of the spongy layer containing a spongy 'coil' (arrow) can be defined. Scale bar denotes (*a*) 10 μm, (*b*) 10 μm, (*c*) 25 μm.

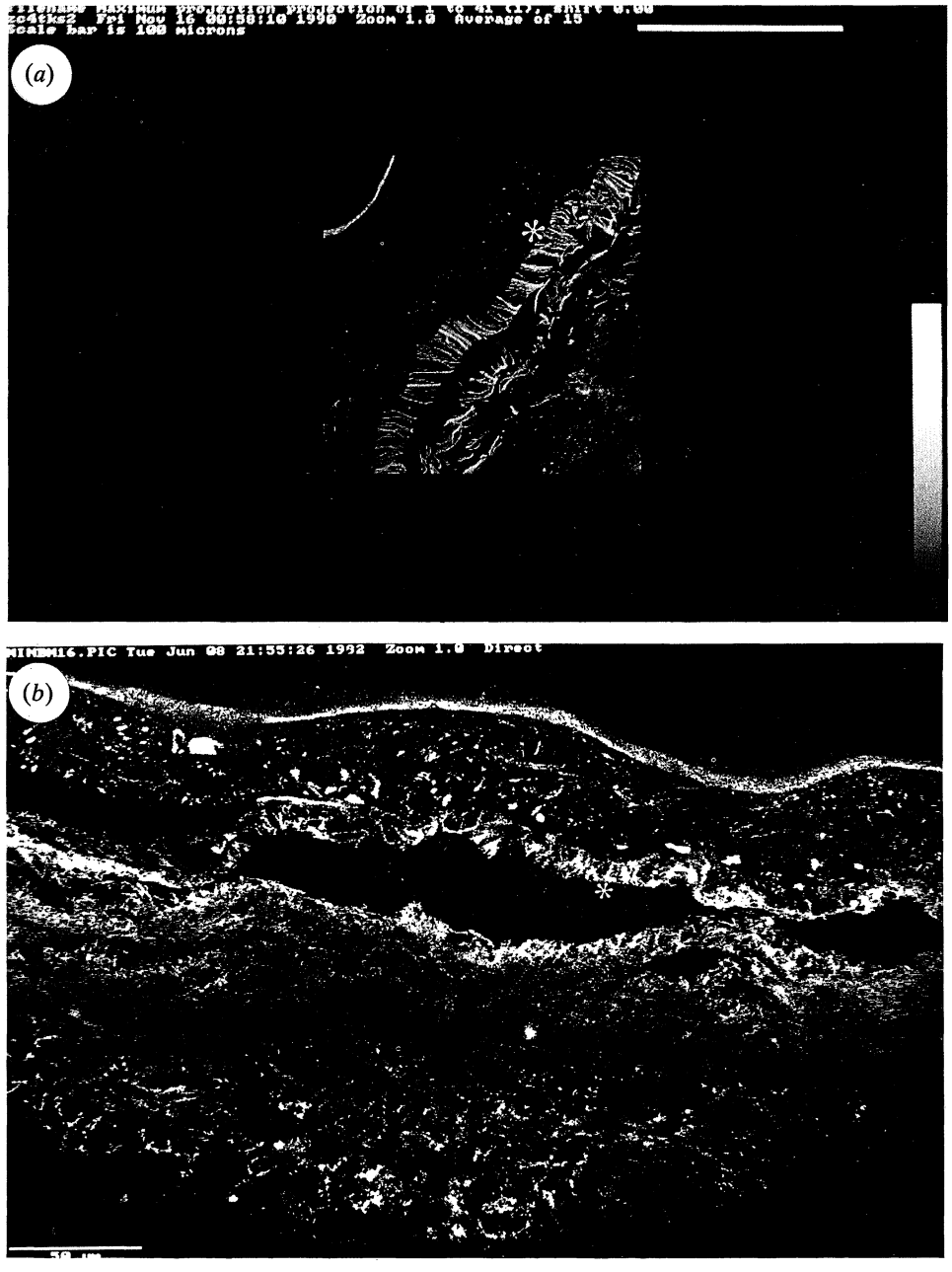

Figure 3. Confocal indirect immunofluorescence micrographs showing the distribution of anti-type IV collagen immunoreactivity. (*a*) Detail showing the 'coil' structures in the spongy layer (asterisks). The thin fluorescent bright line of the amniotic epithelial basement membrane can be seen at top left. (*b*) Here two 'coils' in the spongy layer can be seen which have separated over part of their length (asterisks). Scale bar denotes (*a*) 100 μm, (*b*) 50 μm.

trated over moderately electron dense areas with a texture typical of that seen in other basal laminae in electron micrographs. The distribution of the colloidal gold particles marking the location of type IV collagen at the ultrastructural level parallels the distribution of the anti-type IV collagen immunofluorescence observed in the light microscope. Labelling of the amniotic epithelial basement membrane is shown by figure 9*a* and control by figure 9*b*. Labelling of the chorion laeve (pseudobasement) membrane is shown in figures 10*a* and 11*a*,*b* and not by the control figure 10*b*. Labelling of the extracellular matrix between trophoblast cells also occurs. Labelling of regions within the connective tissue layers distant from base-

Figure 4. Confocal indirect immunofluorescence micrograph showing the distribution of anti-type IV collagen immunoreactivity. (*a*) This gallery of images shows a series of images of projections through a voxel array formed from serial optically sectioning on the *z*-axis through coil elements in the spongy layer. The views presented are those which would be seen if the solid image were rotated by equal steps through 360°. At the appropriate orientation the coils appear to be separate. (*b*) Orthogonal rotation showing the curvature of fibres in the coils. Scale bars denote 100 μm.

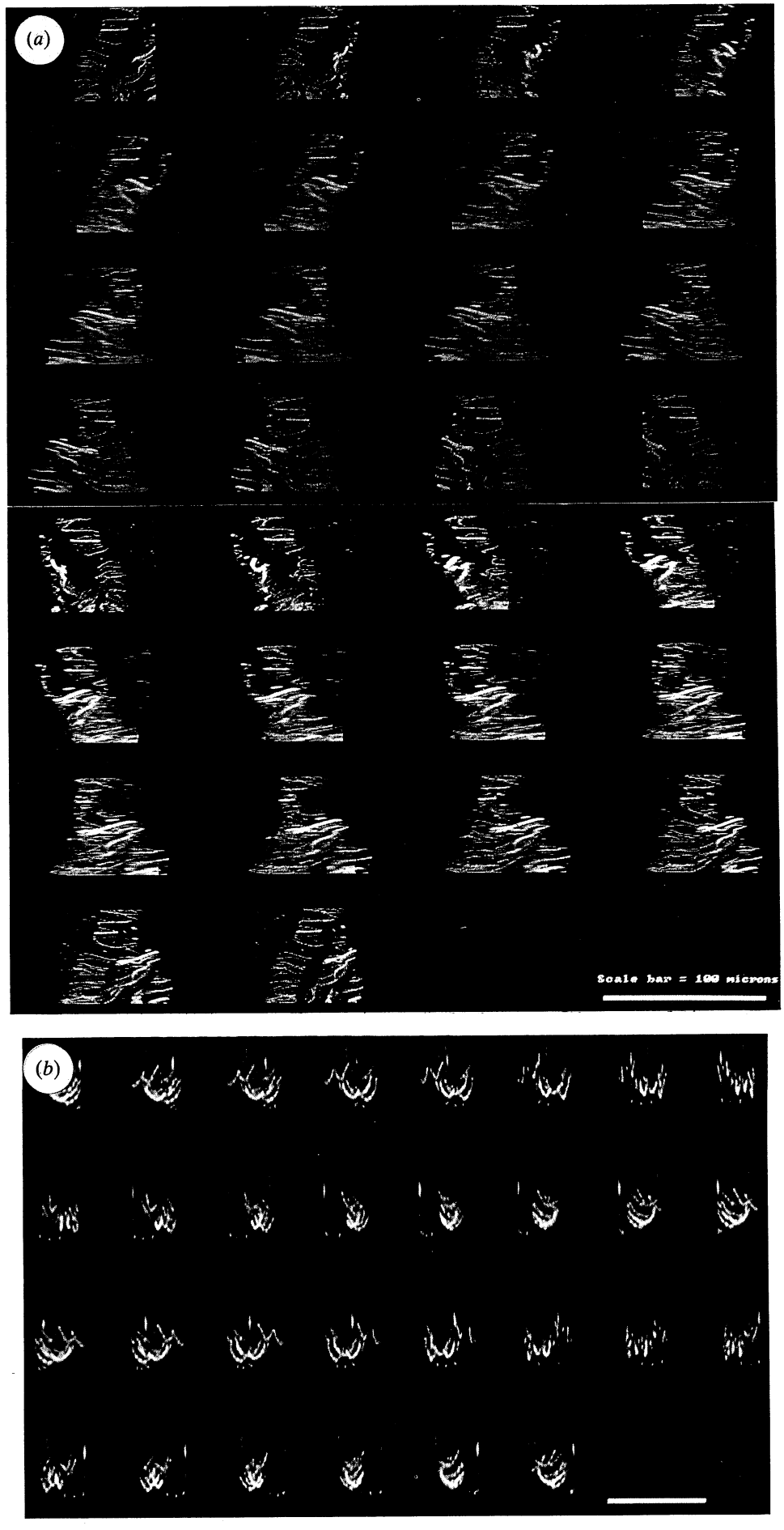

Figure 4. For description see opposite.

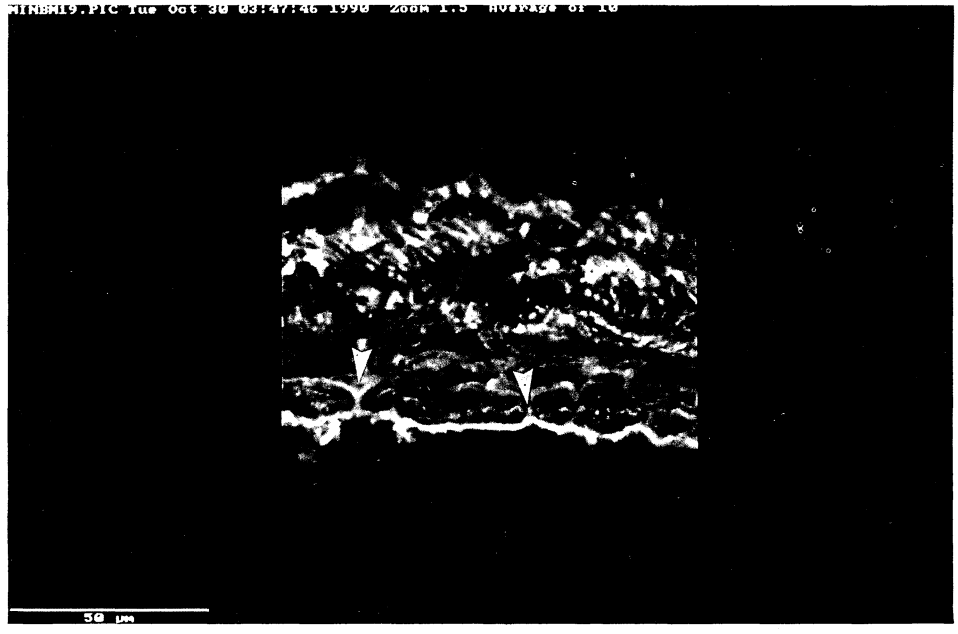

Figure 5. Confocal indirect immunofluorescence micrograph showing the distribution of anti-type IV collagen immunoreactivity. Here the trophoblastic basement membrane ('pseudobasement') membrane is clearly defined. There is some reactivity extending up through the reticular layer into the spongy layer. Note the immunoreactive connections at the interface (arrows). Scale bar denotes 50 μm.

ment membranes is shown in figure 11*a*,*b*. In all of these cases the underlying texture of the structures are of similar electron density and texture to the lamina densa of a typical basal lamina. Decidual layer blood vessel walls are also associated with immunoreactivity (figure 12).

In connective tissue, structures with the size and shape of the micro-trabeculae observed with the immunofluorescence microscope were also observed with the electron microscope. These exhibited the same electron density and ultrastructure as the lamina densa of the amniotic epithelial basement membrane. The structures appeared to be associated with relatively long strands of fibrous collagen which are generally sparsely distributed in the tissue at these levels (figure 11*a*,*b*).

The specific immunolocalization with colloidal gold frequently resulted in small clusters of electron dense particles over features with similar ultrastructural appearance. We believe that this relates to the pattern of exposure of antigenic sites at the surface of the resin section (see Discussion).

(*b*) *Laminin*

Using the anti-laminin antibody, fluorescence above background levels was associated with the following extracellular matrix components: amniotic epithelial basement membrane; trophoblastic epithelial ('pseudo-') basement membrane; trophoblast layer extracellular matrix; spongy layer; walls of decidual blood vessels. In the reticular layer, specific immunofluorescence was faint. Within the fibroblast layers, isolated trabecular structures exhibited positive fluorescence (figure 6*a*,*b*). Anti-laminin immunoreactivity was frequently associated with the presence of type IV collagen as revealed by dual immunofluorescence (figures 6*a*,*b* and 8*c*).

In several indirect immunofluorescence preparations using the anti-laminin antibodies the presence of a narrow zone of reduced fluorescence intensity on the reticular layer side of the chorion laeve basement membrane was noted (figure 6).

Islands of tissue within the chorion laeve trophoblast were observed which showed the morphological characteristics of 'degenerate villi'. An anti-laminin immunoreactive layer with the same dimensions as the layer in the nearby chorion laeve basement membrane was observed surrounding it (figure 6*b*).

(*c*) *Nidogen*

Using the anti-nidogen antibody, fluorescence above background levels was associated with a similar range of extracellular matrix components: amniotic epithelial basement membrane; chorion laeve ('pseudo-') basement membrane; chorion laeve trophoblast layer extracellular matrix; spongy layer; walls of decidual blood vessels. In the reticular layer immunofluorescence was faint. Within the fibroblast layers, isolated trabecular structures which exhibited positive fluorescence were observed (figure 7*a*,*b*). These were similar in appearance to the structures which were immunoreactive with anti-type IV collagen and anti-laminin as shown by dual labelling (figure 8*c*).

One point of note in several indirect immunofluorescence preparations using the anti-nidogen antibodies was the presence of a narrow zone of reduced fluorescence intensity on the reticular layer side of the

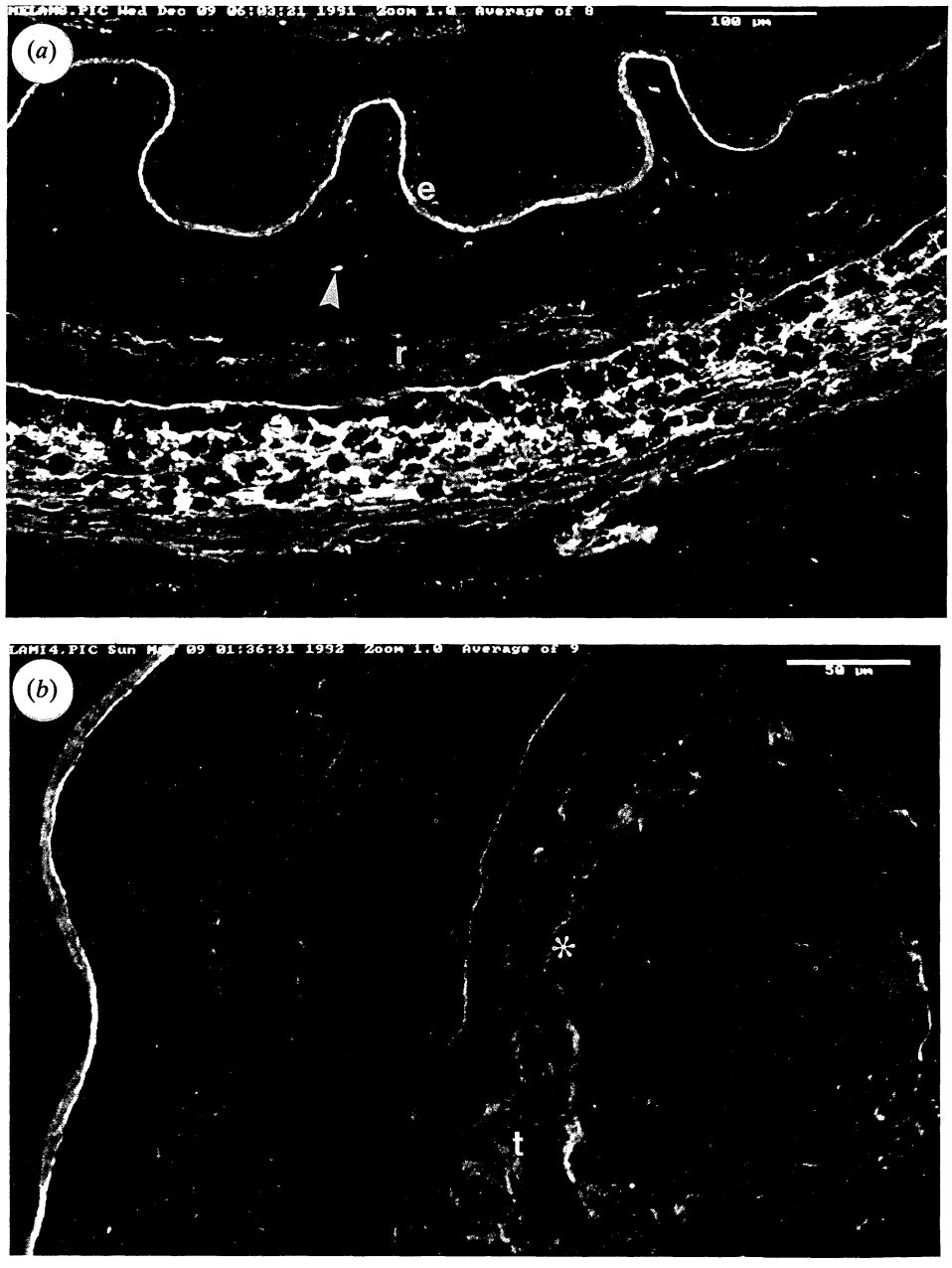

Figure 6. (*a*) Confocal indirect immunofluorescence micrograph showing the distribution of anti-laminin immunoreactivity. The pattern is very similar to that of type IV collagen. There is strong fluorescence in the amniotic epithelial basement membrane (e) and the trophoblast layer and its basement membrane (asterisk), and relatively weak fluorescence in the reticular layer (r). The trabeculae in the fibroblast layer are immunoreactive (arrow). (*b*) This anti-laminin indirect immunofluorescence confocal micrograph shows there is immunoreactivity in a narrow layer surrounding the apparent islands of tissue found within the trophoblast. This is an appearance consistent with the fact that a basement is present at this interface (asterisk). Scale bar denotes (*a*) 100 µm, (b) 50 µm.

chorion laeve basement membrane. This was crossed by strands of anti-type IV collagen reactive matrix as demonstrated by immunofluorescence and immunoelectron microscopy (figures 5, 7*a* and 10*a*).

(*d*) *Fibronectin*

The pattern of immunoreactivity with anti-fibronectin was much more homogeneous throughout the tissue than was that of immunoreactivity with type IV collagen, laminin and nidogen (figure 8*a*). There was a more intense reaction in the compact layer where labelling with the other three antibodies was minimal. Dual label study by anti-laminin and anti-fibronectin make this explicit (figure 8*b*). In several sections bright anti-fibronectin specific fluorescence was observed associated with laminae within the spongy layer. In some regions these laminae were associated with cleavage planes between amnion and chorion.

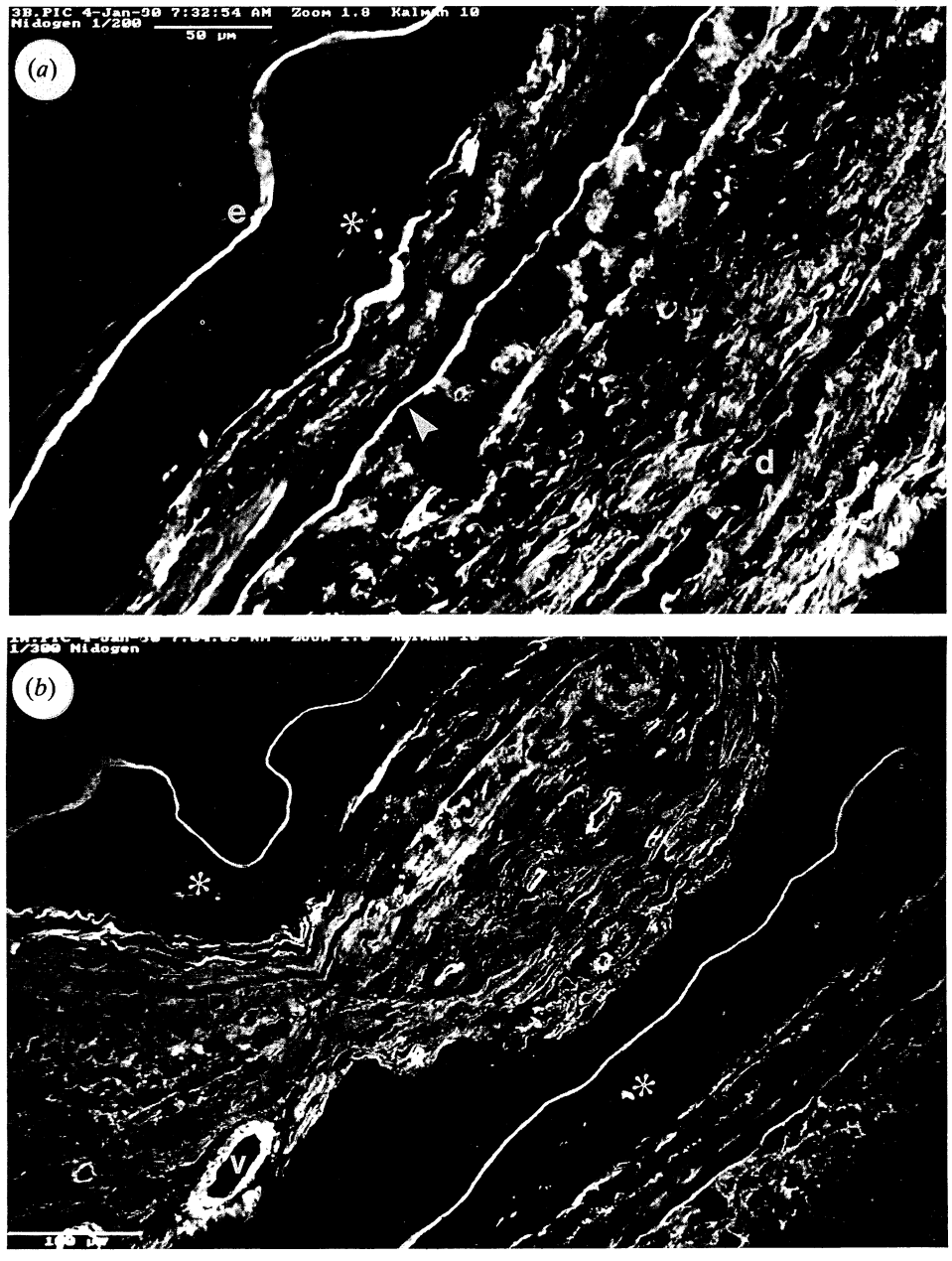

Figure 7. Confocal indirect immunofluorescence micrograph showing the distribution of anti-nidogen immunoreactivity. The immunoreactivity pattern is very similar to that of the type IV collagen and laminin. (*a*) There is strong fluorescence in the amniotic epithelial (e) and trophoblastic basement membrane (arrow) as well as in the decidua (d). The trabeculae in the fibroblast layer are strongly immunoreactive (asterisk). (*b*) Decidual blood vessels reveal intense specific immunofluorescence in vessel walls coincident with endothelial basement membranes (v). The trabeculae in the fibroblast layer are strongly immunoreactive (asterisk). Scale bar denotes (*a*) 50 µm, (*b*) 100 µm.

4. DISCUSSION

The evidence presented indicates the presence of short segments or trabeculae in the extracellular matrix of the human amnion. These structures appear to contain type IV collagen, laminin and nidogen and thus share compositional characteristics with basal laminae and anchoring plaques (Keene *et al.* 1987). They also share some of the histological and ultrastructural characteristics of lamina densa of basal laminae and

PLATE 1

Figure 8. (*a*) Confocal indirect anti-fibronectin immunofluorescence micrograph of human fetal membrane at term. Note the immunofluorescence in the compact layer (asterisk), at cleavage planes (arrow), and the low level of distributed fluorescence throughout the tissue including the compact layer. Scale bar denotes 50 µm. (*b*) Dual immunofluorescence micrograph showing the disposition of anti-laminin immunoreactivity (green channel) and anti-fibronectin immunoreactivity (red channel). Scale bar denotes 50 µm. (*c*) Dual immunofluorescence micrograph showing the disposition of anti-type IV collagen immunoreactivity (red channel) and anti-laminin immunoreactivity (green channel). Scale bar denotes 50 µm.

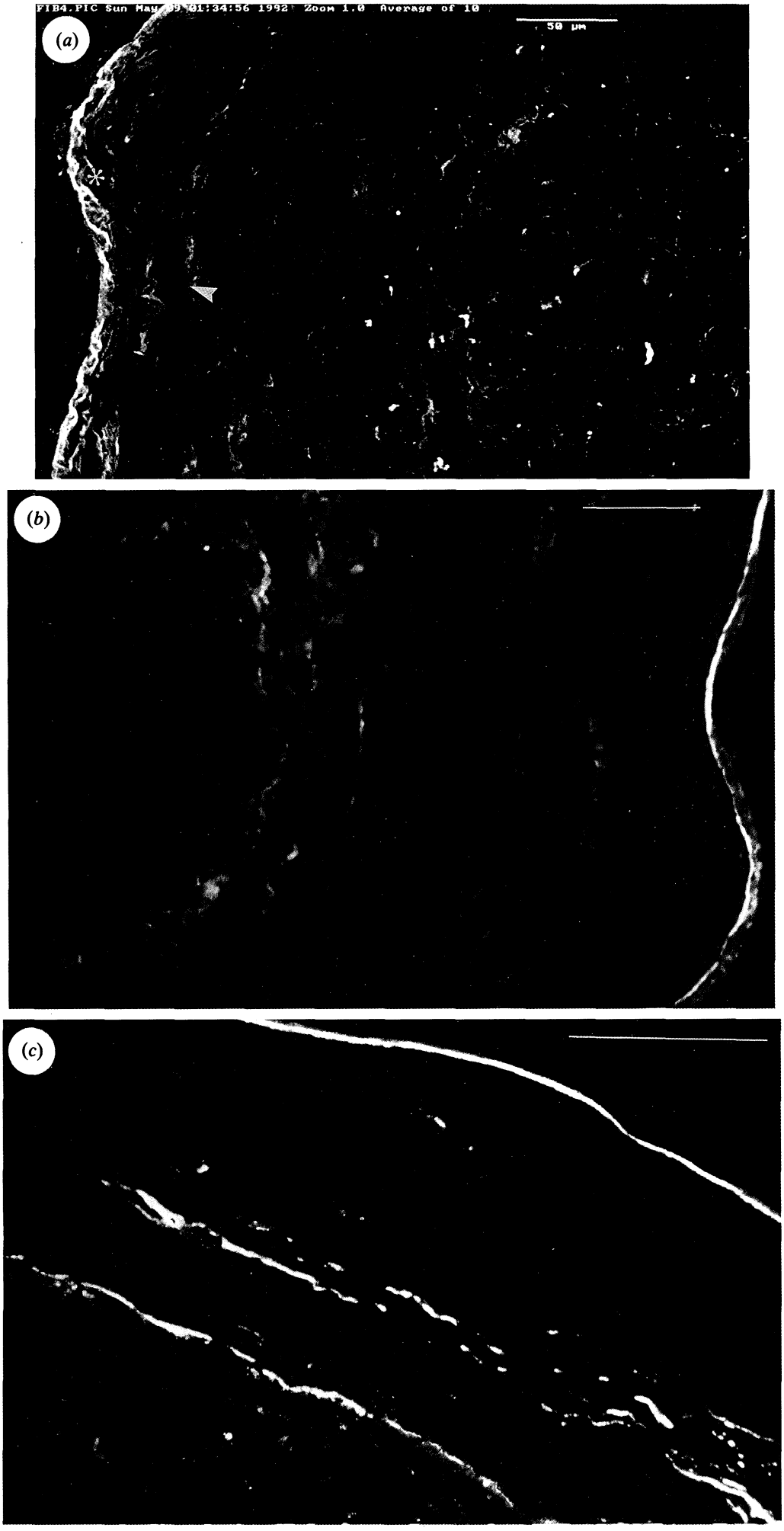

Figure 8 *a–c*. For description see opposite.

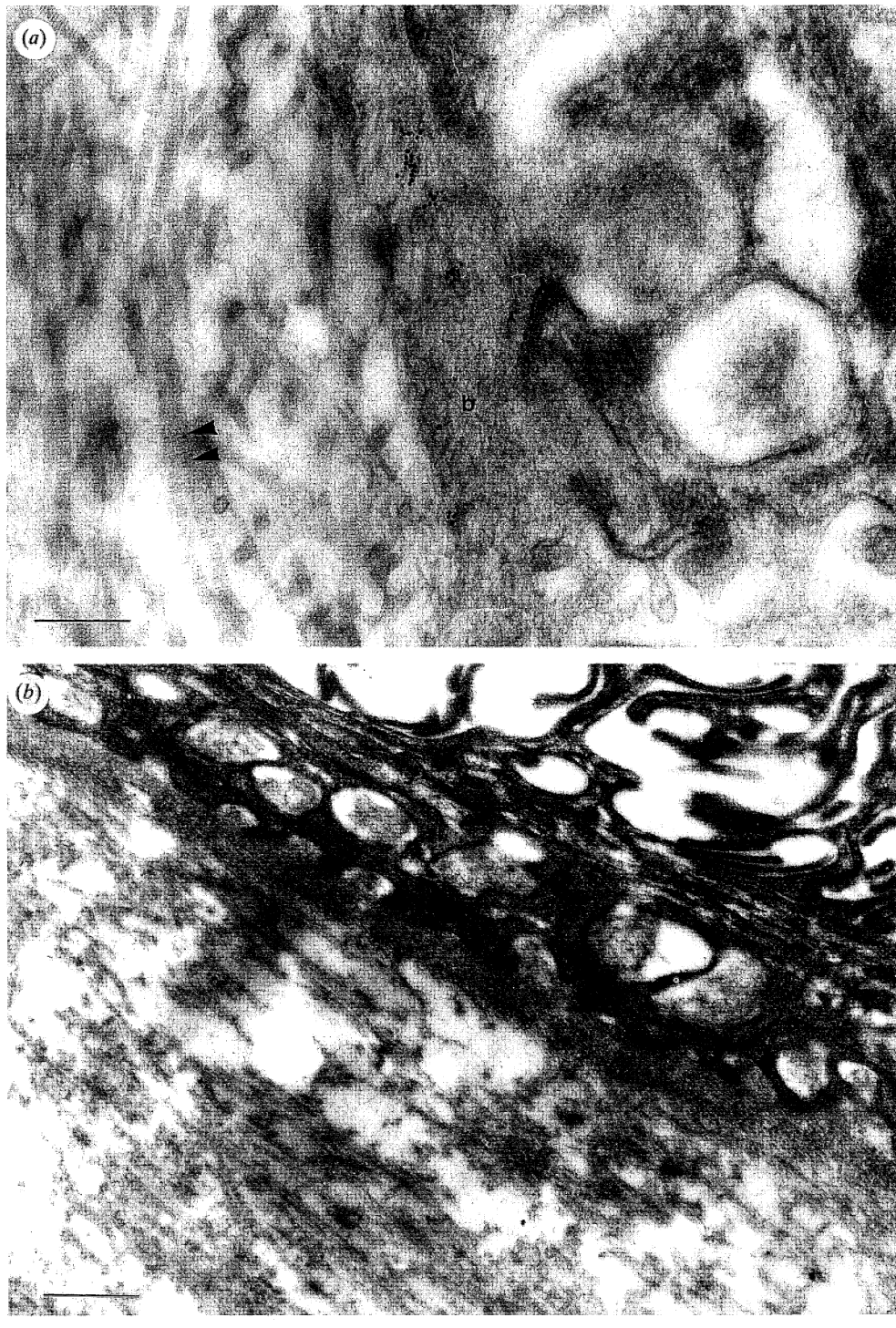

Figure 9. (*a*) Electron micrograph of low-temperature, low-denaturation embedded tissue. The electron dense colloidal gold particles reveal the sites immunoreactive with anti-IV collagen. In this field labelling is restricted to the amniotic epithelial basement membrane (b). Note the absence of label over the banded collagen fibres of the compact layer (arrows). (*b*) A similar field from a control preparation in which the sites were blocked with an excess of unlabelled antibody to show the background level of labelling. Scale bars denote (*a*) 0.2 μm, (*b*) 0.5 μm.

anchoring plaques (Keene *et al.* 1987). The micro-trabeculae are clearly dissimilar from both of these other structures on grounds of composition, location and size; they may, however, be related to them in some as yet undefined way.

Presently the origin and function of these structures are obscure. However, it may be important that the spongy layer close to which the micro-trabeculae are found originates from the extraembryonic coelom and is thus not embryologically part of either the amnion or chorion (figure 13). This study has been performed exclusively using term tissue. By this stage of development the cellular layer, which forms the boundary between the spongy layer and the reticular layer, is

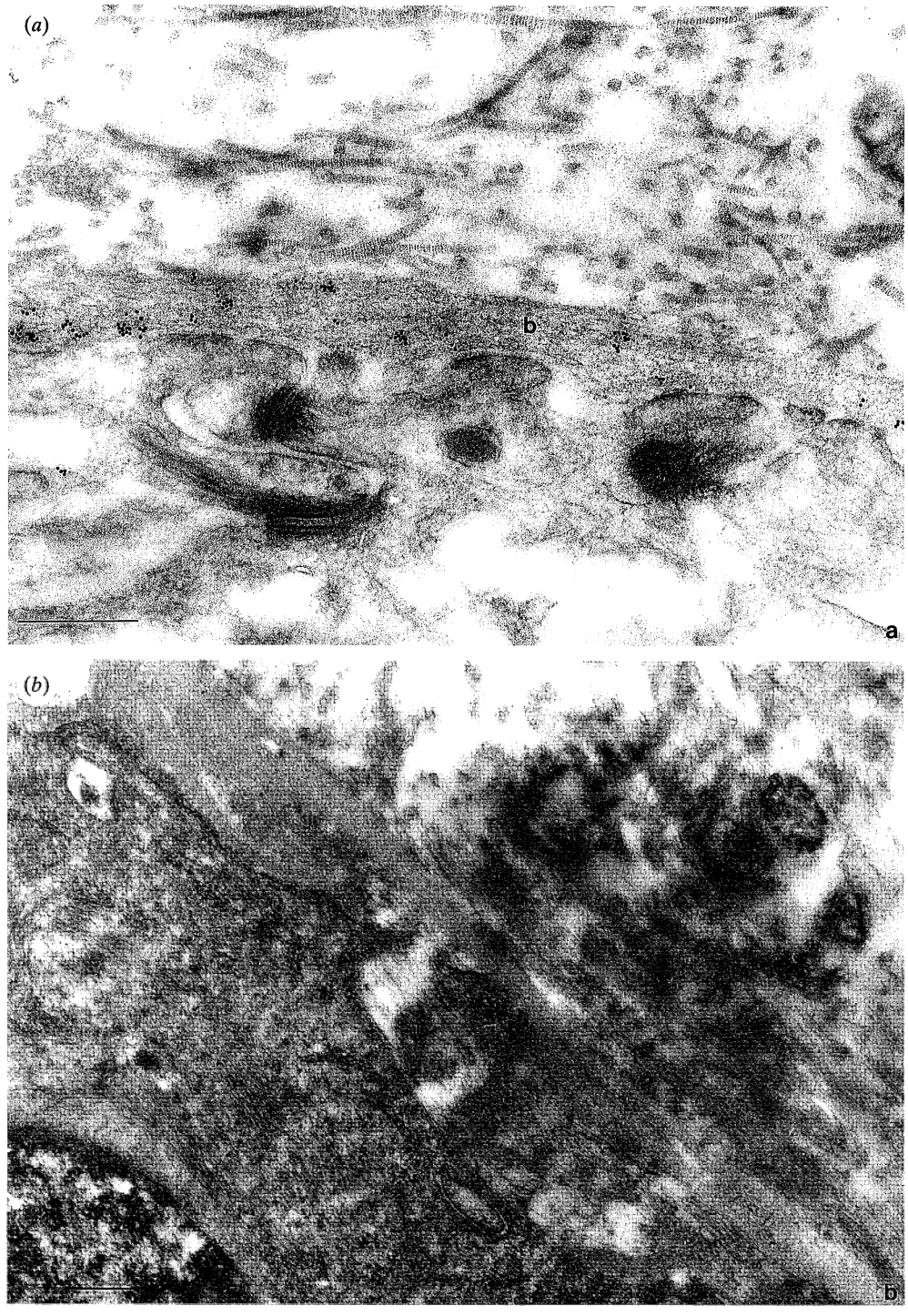

Figure 10. (*a*) Electron micrograph of low-temperature, low-denaturation embedded tissue. The electron dense colloidal gold particles reveal the sites immunoreactive with anti-type IV collagen. In this field labelling is restricted to the basement membrane (b) of the trophoblastic epithelium. (*b*) A similar field from a control preparation in which the immunoreactive sites were blocked with an excess of unlabelled antibody. Scale bars denote (*a*) 0.5 μm, (b) 0.5 μm.

usually absent. Earlier it is a consistent but simple unicellular layer. The possibility exists therefore that these elements are embryological remnants of a basal lamina of this layer. This possibility, however, is a slim one as the cellular layer is found in association with the reticular layer not the fibroblast layer, and one would have to suggest that most trabeculae or trabecular components had migrated to this new site.

If at one time associated with an 'epithelial' layer, as is typical of the lamina densa of a basal lamina, the structure would be expected to be continuous. Controlled disassembly during the regression of a previously functional and continuous sheet might be expected to lead to numerous fairly widely spaced segments of similar lengths.

What epithelial-like structures are present in the conceptus at earlier stages? The most obvious is Heuser's membrane which delaminates from the

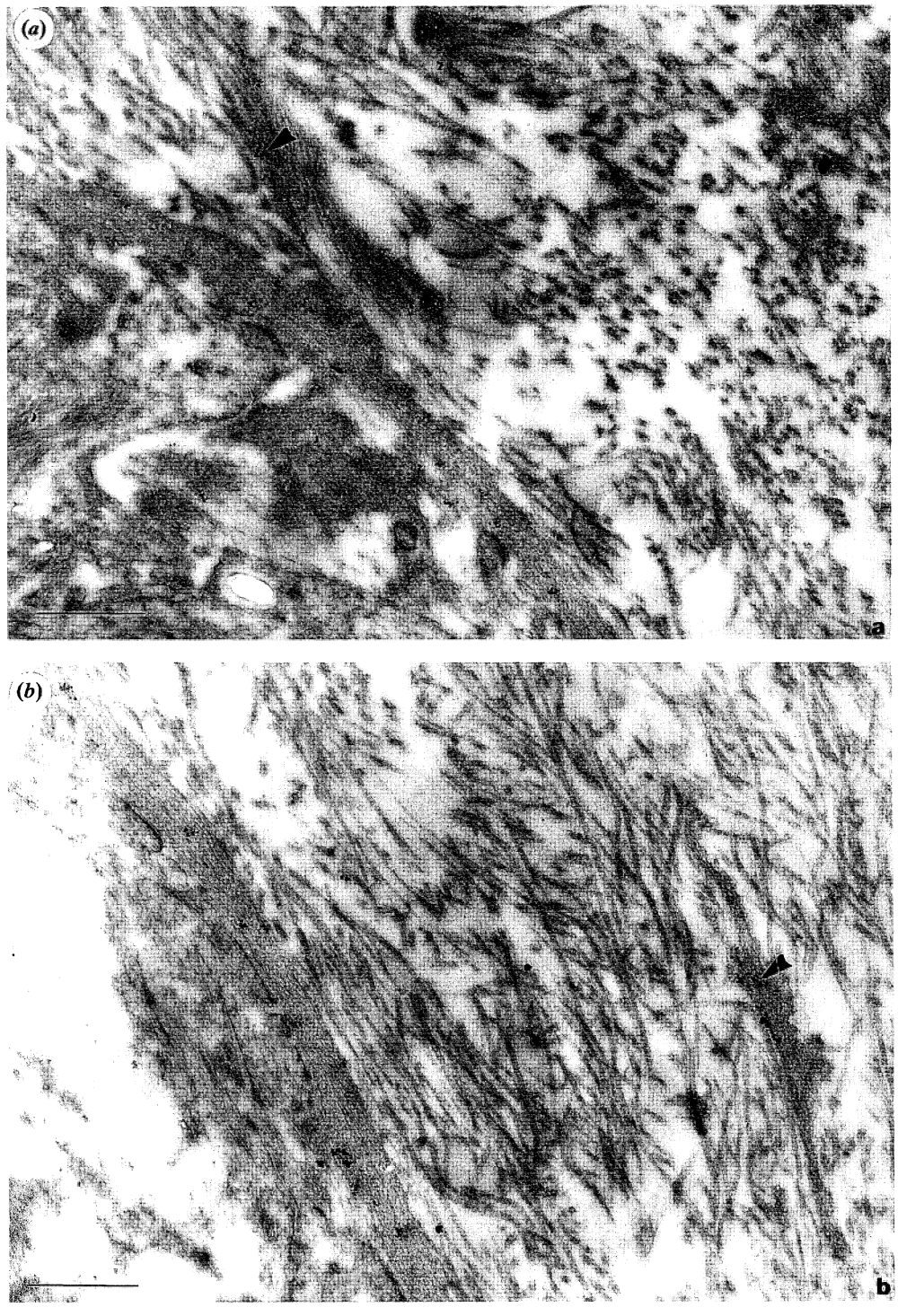

Figure 11. (*a*) Electron micrograph of low-temperature, low-denaturation embedded tissue taken from the site where the chorion laeve contacts the reticular layer. The electron dense colloidal gold particles reveal the sites immunoreactive with anti-type IV collagen. Note the strand of basement membrane-like material reaching out from the chorion laeve basement membrane into the neighbouring reticular layer connective tissue (arrow). Compare this with the structures seen at the light microscope level shown in figure 5 which also demonstrate anti-type IV collagen immunoreactivity. (b)Electron micrograph of low-temperature, low-denaturation embedded tissue taken from the site where the chorion laeve contacts the reticular layer. The electron dense colloidal gold particles reveal the sites immunoreactive with anti-type IV collagen. In this field labelling is restricted to the basement membrane and basement membrane-like material found in the reticular layer connective tissue (arrow). Scale bars denote (*a*) 0.5 μm, (*b*) 0.5 μm.

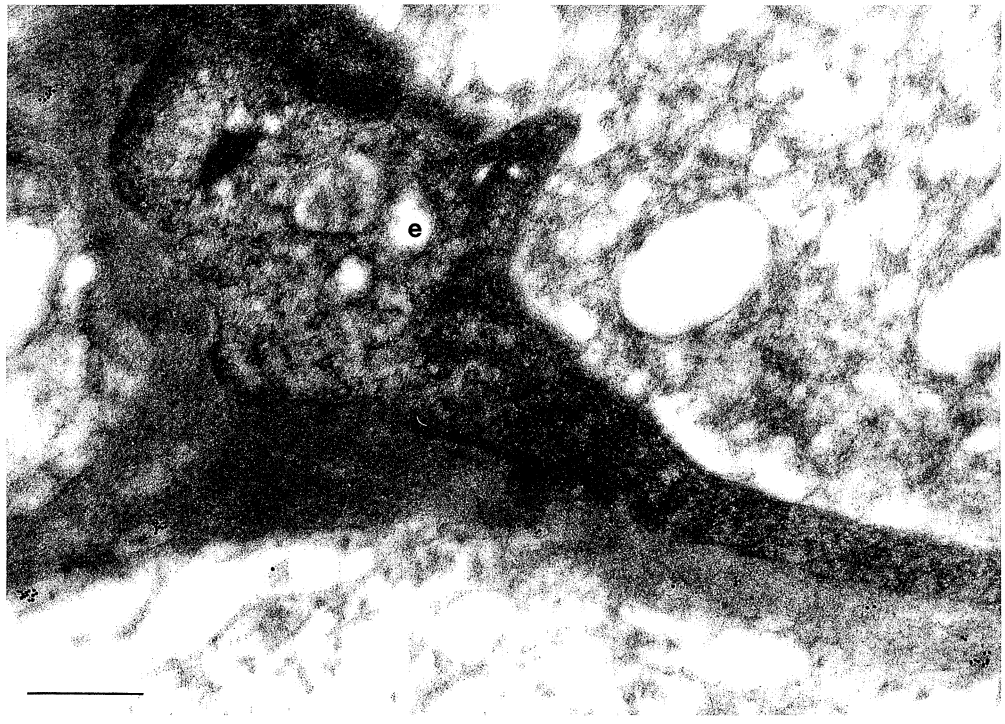

Figure 12. Electron micrograph of low-temperature, low-denaturation embedded tissue. The electron dense colloidal gold particles reveal the sites immunoreactive with anti-type IV collagen. In this field labelling is restricted to the endothelial basement membrane adjacent to a decidual capillary endothelial cell (e). Scale bar denotes 0.3 μm.

mural trophobastic cells to form the wall of the primary yolk sac. This structure, however, becomes restricted to a small part of the conceptus at an early stage. At a slightly later stage, although poorly documented, cells of the extraembryonic coelom group together to form fluid filled lakes which eventually coalesce to form the extraembryonic coelom. This coelom and presumably its boundary walls extend over the full surface of the interface between the amnion and chorion with the exception of the body stalk (later the umbilical cord). Oedematous blisters forming planes separating spongy layer tissue can be seen in many locations in term amniochorion. It is not known whether these are entirely formed *de novo* or whether they depend on surviving structures once important as coelom generators.

Alternatively, it is now appreciated that type IV collagen-containing structures are not restricted to basal laminae and therefore the environment of an epithelium (Pratt & Madri 1985; Nanaev *et al.* 1991). Extracellular matrix plaques containing type IV collagen may act as terminal cross-linkers which help to integrate the mechanical network of fibrous collagen at points distant from a basal lamina (Keene *et al.* 1987). This has been demonstrated to be the case for type VII collagen which is known to form minute anchoring fibrils at the dermo-epidermal junction (Sakai *et al.* 1986).

A typical basement membrane of differentiated tissue contains the following components; collagen IV, laminin, nidogen, BM40 and proteoglycans (Martin & Timpl 1987). Fibronectin is found in embryonic basement membranes (Alitalo *et al.* 1980), and banded type I and III collagen fibres are seen where a lamina reticularis is present. A range of these components should be investigated to define the composition of these structures. Laminin is thought to be a typical component of basement membrane (Farquhar 1981), and its presence has been confirmed in human fetal membranes (Klima & Schmidt 1988). The demonstration of typical basement membrane components in the discrete structures present in the fibroblast layer in the present experiments confirms that the structures have much in common with basement membranes.

(*a*) *Laminae reticularis*

A region of low immunofluorescence with anti-collagen type IV, anti-nidogen and anti-laminin antibodies was found on the reticular side of the chorion laeve 'pseudo'-basement membrane. This may represent a lamina reticularis. A conventional basal lamina consists of three ultrastructurally distinct layers: lamina lucida, lamina densa and lamina reticularis. The latter is fibrous and links the basal lamina to the fibrous elements of neighbouring connective tissues. The immunofluorescence 'hiatus' first observed by J. Smith (personal communication) and described here may represent this feature which is another sign of the authenticity and typical nature of the misnamed 'pseudo'-basement membrane.

The compact layer of the amnion is unique in containing no demonstrable sites with any immunoreactivity to anti-IV collagen/laminin and nidogen. This layer which is thought to be responsible for a great deal of the strength of the tissue contains no cells whatsoever. It is unusual because its matrix composition containing apart from the fibronectin described

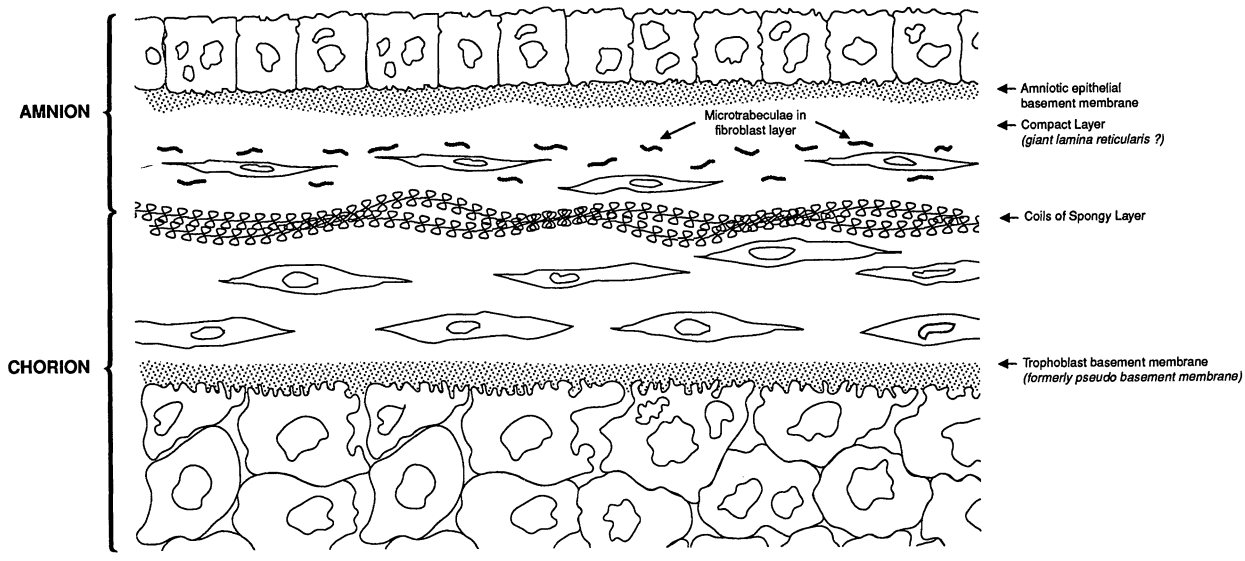

Figure 13. Summary diagram showing the location of the structures described in the text.

here close packed collagen I, III, V & VI (Malak *et al.* 1993). In this it differs dramatically from the neighbouring fibroblast layer. It may help to understand this layer if we think of it as an hypertrophic lamina reticularis of the amniotic epithelial basement membrane. If this proves to be the case its massive size suits it as an experimental model system for study of this layer.

(*b*) *Chorion laeve trophoblast basement membrane*

The structure called the 'pseudobasement membrane' (to avoid confusion with the amniotic epithelial basement membrane) by Bourne (1962) appears to be a structurally and compositionally normal embryonic basement membrane associated with the chorion laeve trophoblastic epithelium as defined by six criteria which we have investigated: (i) contains IV collagen; (ii) contains laminin; (iii) contains nidogen; (iv) contains fibronectin; (v) similar ultrastructural appearance to lamina densa of basement membrane; and (vi) possession of lamina reticularis.

We recommend that the use of the term pseudobasement membrane be dropped and that it be replaced by the term chorion laeve trophoblast basement membrane.

Aplin & Campbell (1985) have noted ultrastructurally visible extensions of the chorion laeve trophoblast basement membrane within overlying trophoblast and underlying mesenchyme extracellular space, and we have confirmed this by using ultrastructural immunocytochemistry to show type IV collagen at these sites. They use this as evidence of an atypical organization. In fact other basement membranes considered typical do show similar extensions into surrounding tissue planes (Nanaev *et al.* 1991).

Apparent islands of tissue within the trophoblast layer of the chorion ('degenerate villi') have previously been suggested to be a projection of the neighbouring reticular layer into the trophoblast on the basis of the intermediate filament protein composition of the cells (Ockleford *et al.* 1993). The appearance of an anti-laminin immunoreactive boundary layer to these apparent islands similar to that of the nearby trophoblastic basement membrane shown here is consistent with the previous interpretation and indicates that the entrant reticular tissue is invested with a basement membrane.

(*c*) *Spongy 'coils'*

These structures are intriguing for a number of reasons. They exhibit the least intense anti-type IV collagen immunoreactivity of any of the positive structures described here and are also atypical in that they are clearly fibrillar. Thus an underlying fibrous form of collagen may be ultimately responsible for binding small quantities of the immunoreactive form.

Apposed at the shear and separation plane of the amnion and chorion they may be responsible for maintainance of the tissue's tensile strength whilst accommodating changes in area of either amnion or chorion during growth and deformation. As the surface that the amnion and chorion cover is curved, there is a requirement for movement at the interface under many conditions. Thus a function similar in some respects to that of the loops and hooks of 'Velcro' and two spring fasteners may be associated with these elements of the extracellular matrix of the spongy layer. The amnion and chorion may detach locally to take up a tuck or to allow local growth or expansion prior to reforming contact. Our finding that the adhesive protein fibronectin is concentrated at this shear plane implies that a biochemical as well as a mechanical adhesion mechanism maintains the amnio-chorion interaction.

(*d*) *Colloidal gold labelling*

The clustering of immuno-gold particles over various type-IV collagen containing sites is interesting. It is clearly not the well known artefact flocculation, as

in that situation the particles of colloidal gold are in contact with each other, whereas in this situation they are frequently separated by narrow electron-lucent gaps. Overall the labelling appears relatively sparse. This may reflect the fact that only antigen at the cut surface of the resinous ultrathin section is accessible to the first step antibody and this label is visualized against the summated image of the full depth of the tissue in the section. Gold clusters are not common in the background label, thus clustering relates to the conditions around the target not those related to probe preparation.

The three-stage technique which we have used acts as a means of amplifying the number of gold particles which are ultimately bound to any exposed and labelled epitope. This probably accounts for some of the frequency with which accumulations of particles are seen as opposed to single particles. The second point to make is that type IV collagen molecules contribute to extended networks of molecules in basal lamina. Situations where short chains of gold particles are observed may relate to a series of similar epitopes close to each other and interrelated in this basal lamina mesh being exposed together at the cut surface of the section.

The features newly described in this paper are summarized in the diagram (figure 13).

Dr Rupert Timpl very kindly donated the antiserum to recombinant mouse nidogen. We are grateful to Professor J. MacVicar and Dr T. Malak of the Birthright team and the obstetricians and gynaecologists of the Leicester Royal Infirmary for clinical coordination; we also thank Angela Chorley and Kamlesh Chandarana for artwork, Briony Pullford for statistical analysis, and CEC for support. Birthright and the M.R.C. are funding related projects currently running in our laboratory at Leicester Medical School. We thank the Wellcome Trust for a grant supporting the costs of publishing figure 8.

REFERENCES

Alitalo, K., Kurkinen, M., Vaheri, A., Krieg, T. & Timpl, R. 1980 Extracellular matrix components synthesised by human amniotic cells in culture. *Cell* **19**, 1053–1062.

Aplin, J.D. & Campbell, S. 1985 Immunofluorescence study of extracellular matrix associated with cytotrophoblast of the chorion laeve. *Placenta* **6**, 469–479.

Aplin, J.D., Campbell, S. & Allen, T.D. 1985 The extracellular matrix of human amniotic epithelium: ultrastructure, composition and deposition. *J.Cell Sci.* **79**, 119–136.

Aplin, J.D., Campbell, S., Donnai, P., Bard, J.B. & Allen, T.D. 1986 Importance of Vitamin C in maintenance of the normal amnion an experimental study. *Placenta* **7**, 377–389.

Bradbury, F.M. & Ockleford, C.D. 1990 A confocal and conventional epifluorescence microscope study of the intermediate filaments in chorionic villi. *J. Anat.* **169**, 173–187.

Bourne, G.L. 1962 *The human amnion and chorion*, pp. 5–53, 95–111. London: Lloyds.

Bourne, G. L. 1966 The anatomy of the human amnion and chorion. *Proc. R. Soc. Med.* **59**, 1127–1128.

Campbell, S., Allen, T.D., Moser, B.B. & Aplin, J.D. 1989 The translaminal fibrils of the human amnion basement membrane. *J. Cell Sci.* **94**, 307–318.

Dearden, L. & Ockleford, C.D. 1983 Structure of human trophoblast: correlation with function. In *Biology of Trophoblast* (ed. Y. W. Loke & A. Whyte), pp. 69–109. Amsterdam: Elsevier Science Publishers.

Keene, D.R., Sakai, L.Y., Lunstrum, G.P., Morris, N.P. & Burgeson, R.E. 1987 Type VII collagen forms an extended network of anchoring fibrils. *J. Cell Biol.* **104**, 611–621.

Klima, G. & Schmidt, W. 1988 Immunohistochemical studies of the nature of connective tissue in fetal membranes. *Acta histochemica* **84**, 195–203.

Malak, T.M., Ockleford, C.D., Bell, S.C., Dalgleish, R., Bright, N. & MacVicar, J. 1993 Confocal immunofluorescence localisation of collagen Types I, III, IV, V, and VI and their ultrastructural organization in term human fetal membranes. *Placenta* **14**, 385–406.

Martin, G.R. & Timpl, R. 1987 Laminin and other basement membrane components. *A. Rev. Cell Biol.* **3**, 57–85.

Modesti, A., Kalebic, T., Scarpa, S., Togo, S., Grotendorst, G., Liotta, L. & Triche, T. 1984 Type V collagen in human amnion is a 12 nm fibrillar component of the pericellular interstitium. *Eur. J. Cell Biol.* **35**, 246–255.

Nanaev, A.K., Rukosuev, V.S., Shirinsky, P., Milovanov, A.P., Domogatsky, S.P., Duance, V.C., Bradbury, F.M., Yarrow, P., Gardiner, L., D'Lacey, C. & Ockleford, C.D. 1991 Confocal and conventional immunofluorescent and immunogold electron microscopic localisation of collagen types III and IV in human placenta. *Placenta* **12**, 573–595.

Ockleford, C.D. 1990 *An atlas of antigens*. London: MacMillan Press. New York: Stockton Press.

Ockleford, C.D., Malak, T., Hubbard, A., Bracken, K., Burton, S.-A., Bright, N., Goodliffe, J., Garrod, D. & D'Lacey, C. 1993 Confocal and conventional immunofluorescence and ultrastructural localisation of strength giving components of human fetal membranes. *J. Anat.* **183**. (In the press.)

Ockleford, C.D. & Wakely, J. 1982 The skeleton of the placenta. In *Progress in anatomy*, vol. 2 (ed. R. J. Harrison & V. Navaratnam), pp. 19–47. Cambridge University Press.

Ockleford, C.D., Wakely, J. & Badley, R.A. 1981 Morphogenesis of placental chorionic villi: cytoskeletal, syncytioskeletal and extracellular matrix proteins. *Proc. R. Soc. Lond.* B **121**, 305–316.

Platt, J.L. & Michael, A.F. 1983 Retardation of fading and enhancement of intensity of immunofluorescence by p-phenylene diamine. *J. Histochem. Cytochem.* **31**, 840–842.

Pratt, B. & Madri, M. 1985 Immunolocalization of type IV collagen and laminin in non-basement membrane structures of corneal stroma. *Lab. Invest.* **52**, 650–656.

Sakai, L.Y., Keene, D.R., Morris, N.P. & Burgeson, R.E. 1986 Type VII collagen is a major structural component of anchoring fibrils. *J. Cell Biol.* **103**, 1577–1586.

Received 9 November 1992; revised 22 February 1993; accepted 17 March 1993

The colour plate in this paper was printed by George Over Limited, London and Rugby

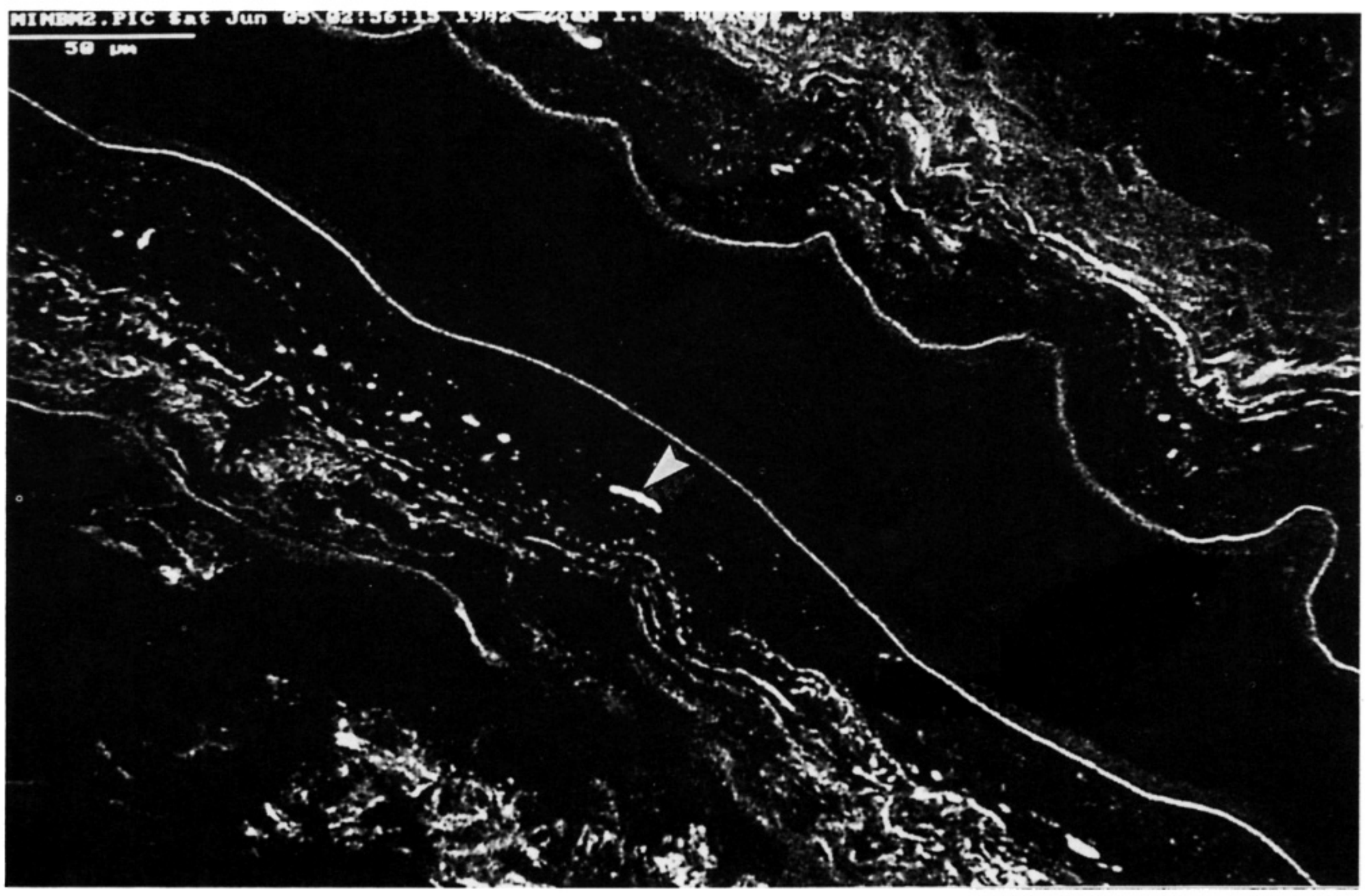

Figure 1. Confocal indirect immunofluorescence micrograph showing the distribution of anti-type IV collagen immunoreactivity. The tissue is folded with the amniotic layers facing inwards along the diagonal from top left to bottom right. The continuous lines of the two amniotic epithelial basement membranes are shown. A series of trabeculae are visible in the fibroblast layer. A particularly large one of these is arrowed.Scale bar denotes 50 µm.

Figure 2. For description see opposite.

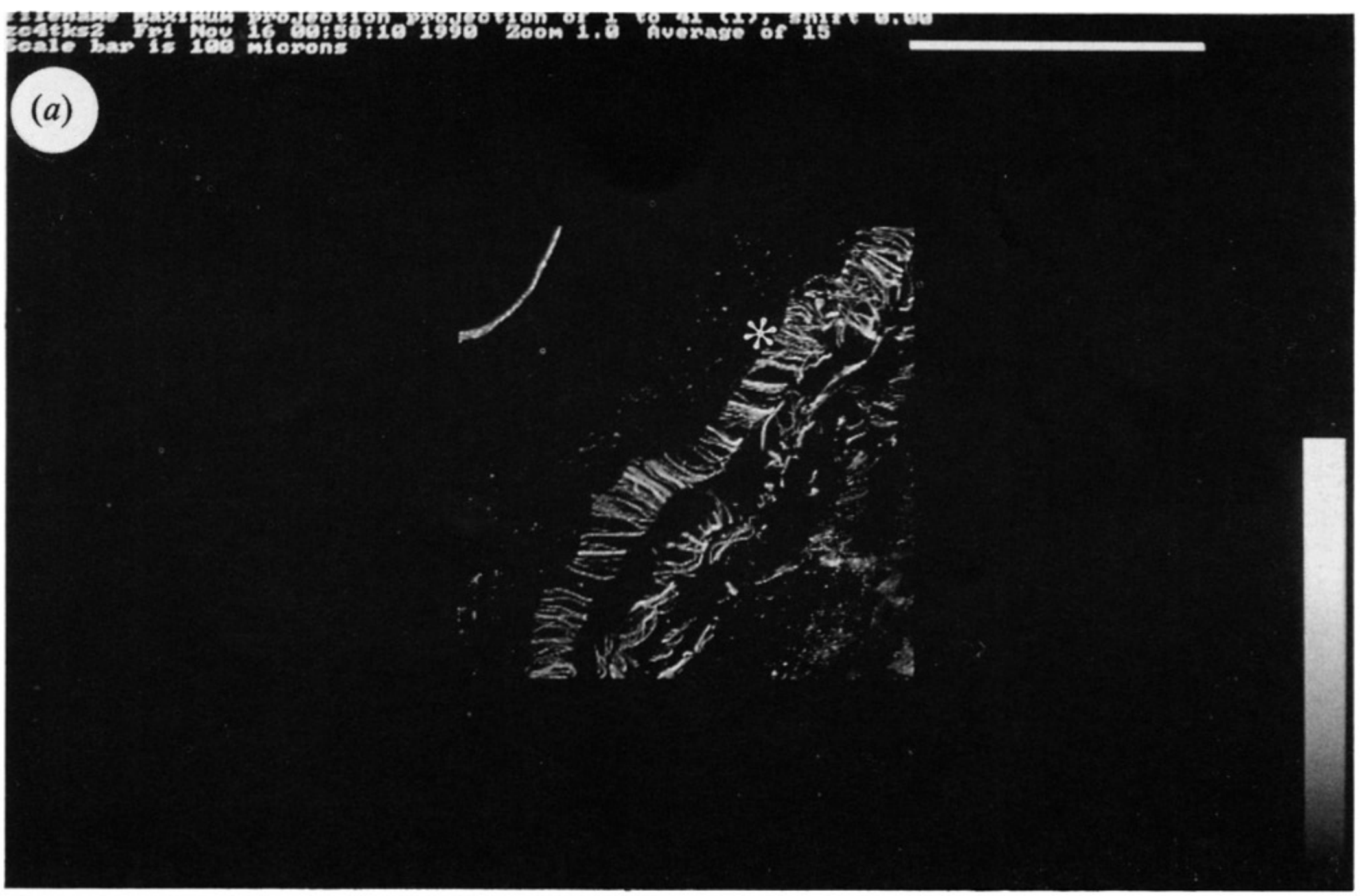

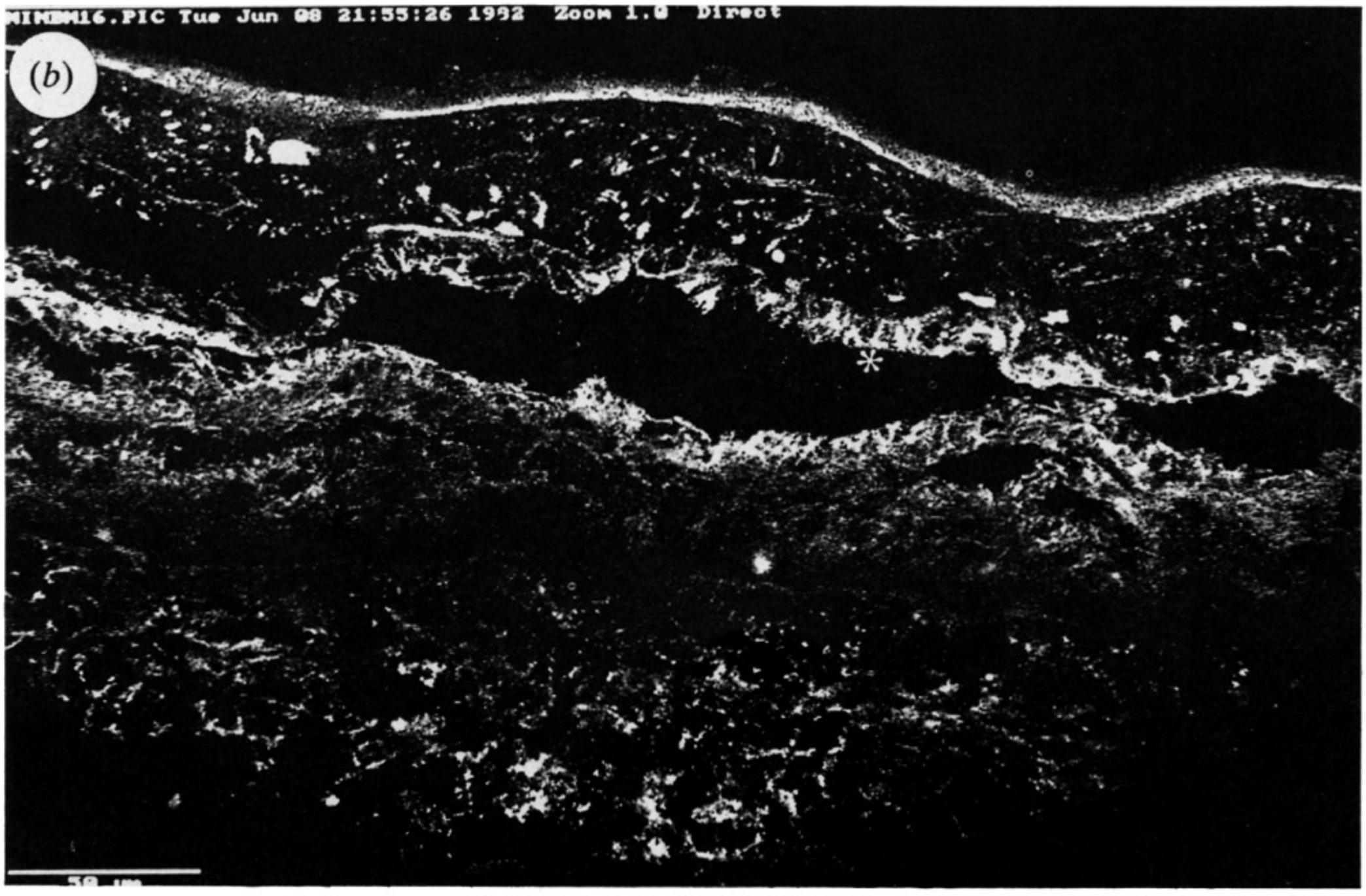

Figure 3. Confocal indirect immunofluorescence micrographs showing the distribution of anti-type IV collagen immunoreactivity. (*a*) Detail showing the 'coil' structures in the spongy layer (asterisks). The thin fluorescent bright line of the amniotic epithelial basement membrane can be seen at top left. (*b*) Here two 'coils' in the spongy layer can be seen which have separated over part of their length (asterisks). Scale bar denotes (*a*) 100 μm, (*b*) 50 μm.

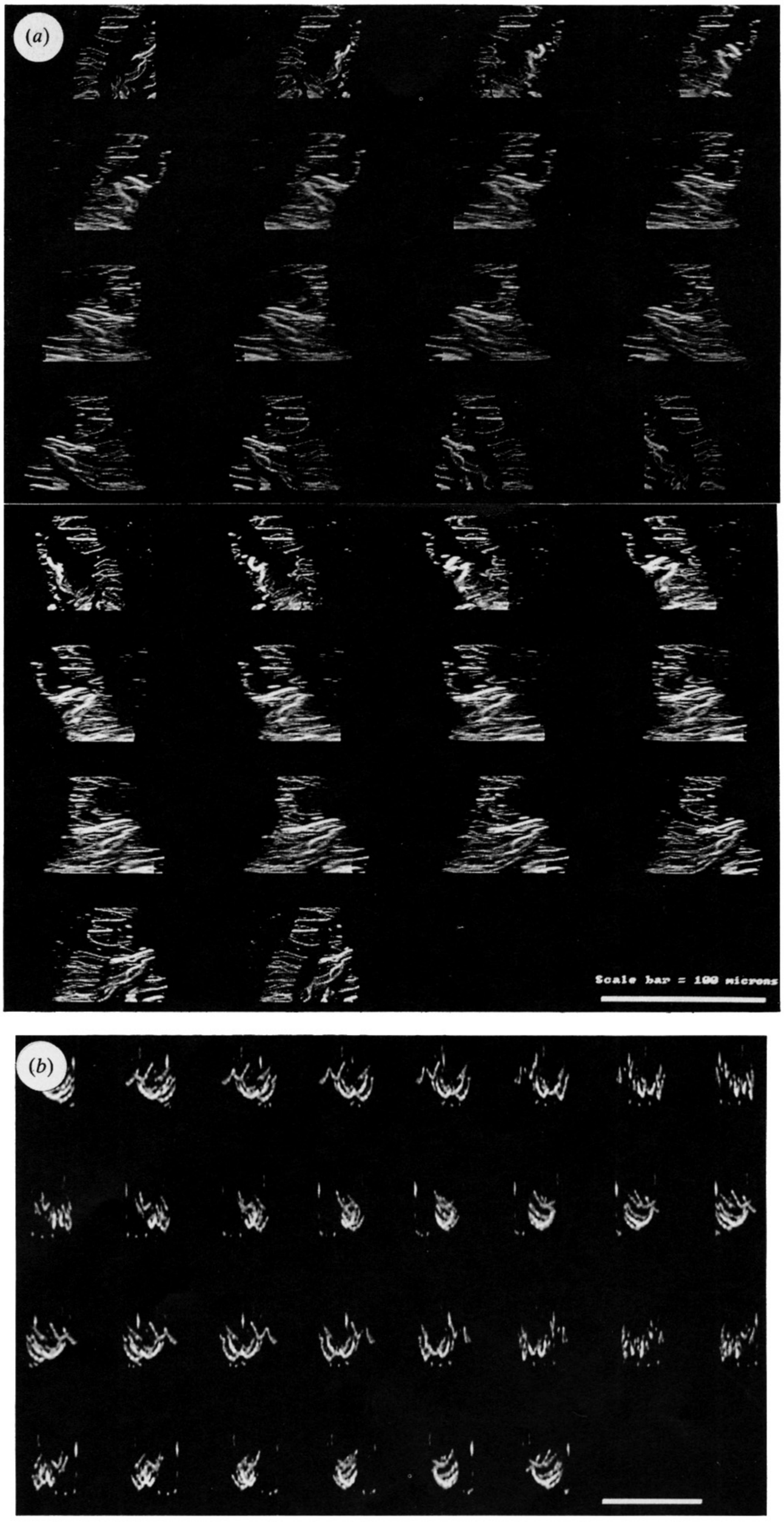

Figure 4. For description see opposite.

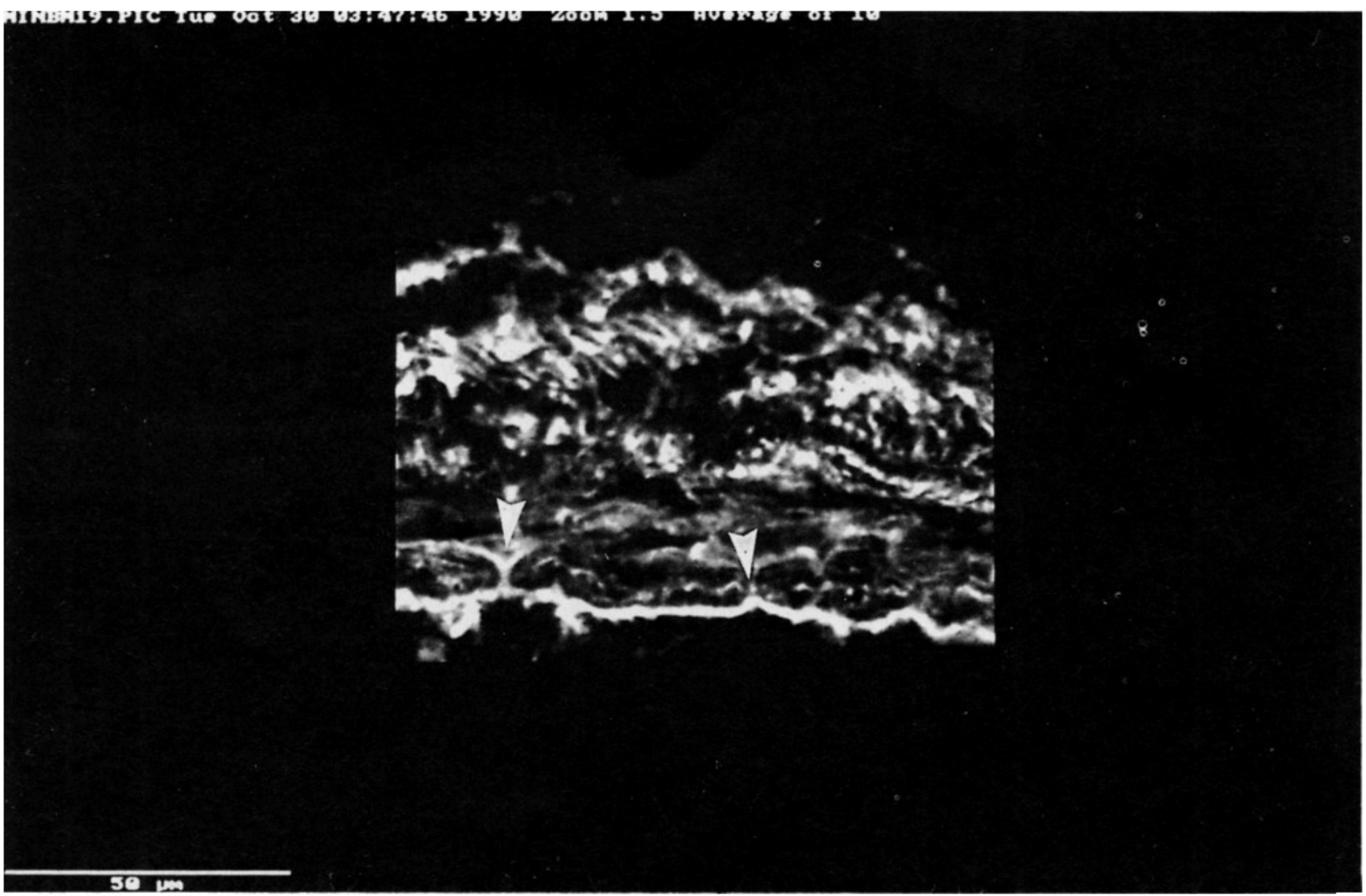

Figure 5. Confocal indirect immunofluorescence micrograph showing the distribution of anti-type IV collagen immunoreactivity. Here the trophoblastic basement membrane ('pseudobasement') membrane is clearly defined. There is some reactivity extending up through the reticular layer into the spongy layer. Note the immunoreactive connections at the interface (arrows). Scale bar denotes 50 µm.

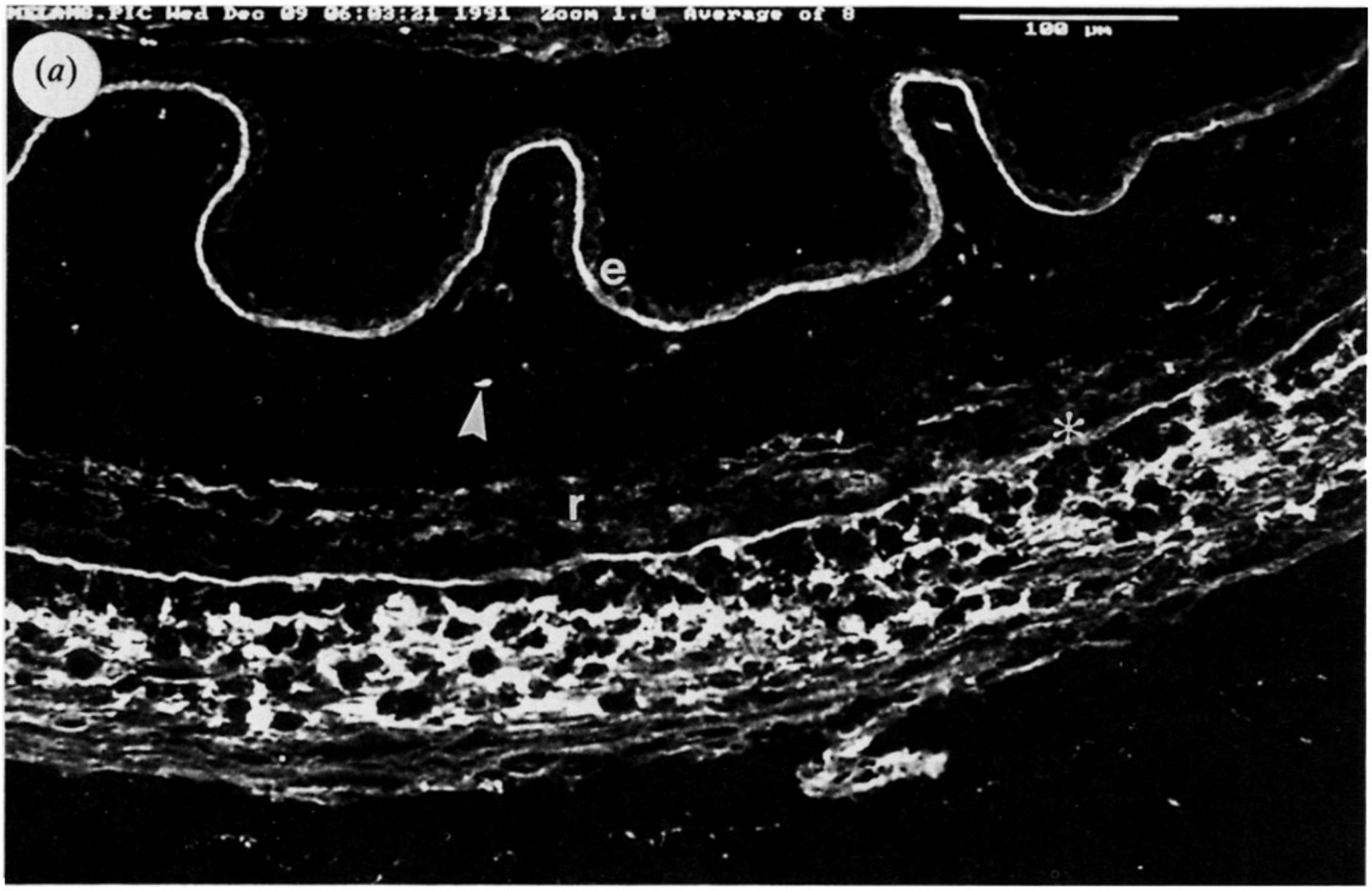

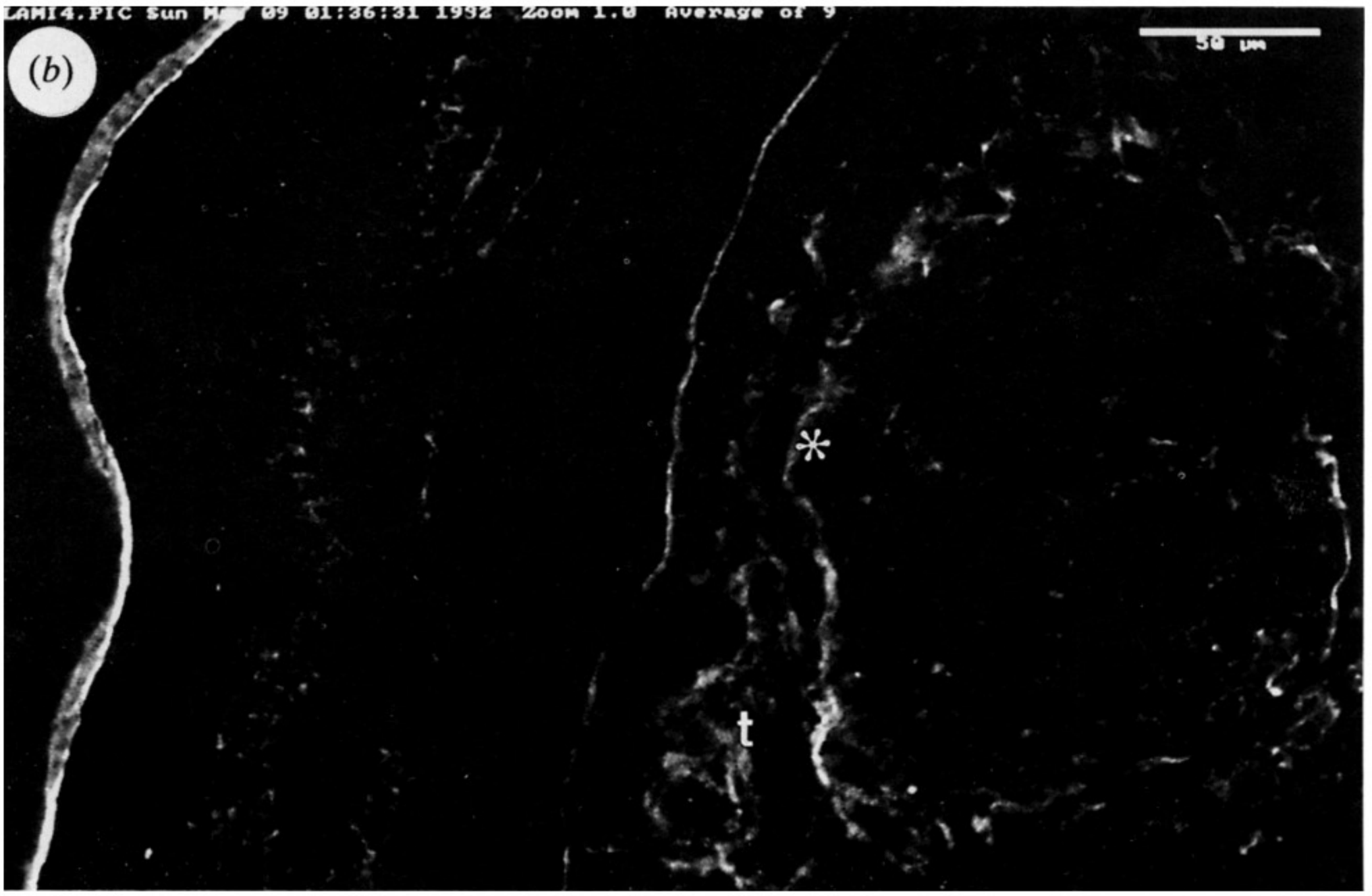

Figure 6. (*a*) Confocal indirect immunofluorescence micrograph showing the distribution of anti-laminin immunoreactivity. The pattern is very similar to that of type IV collagen. There is strong fluorescence in the amniotic epithelial basement membrane (e) and the trophoblast layer and its basement membrane (asterisk), and relatively weak fluorescence in the reticular layer (r). The trabeculae in the fibroblast layer are immunoreactive (arrow). (*b*) This anti-laminin indirect immunofluorescence confocal micrograph shows there is immunoreactivity in a narrow layer surrounding the apparent islands of tissue found within the trophoblast. This is an appearance consistent with the fact that a basement is present at this interface (asterisk). Scale bar denotes (*a*) 100 µm, (b) 50 µm.

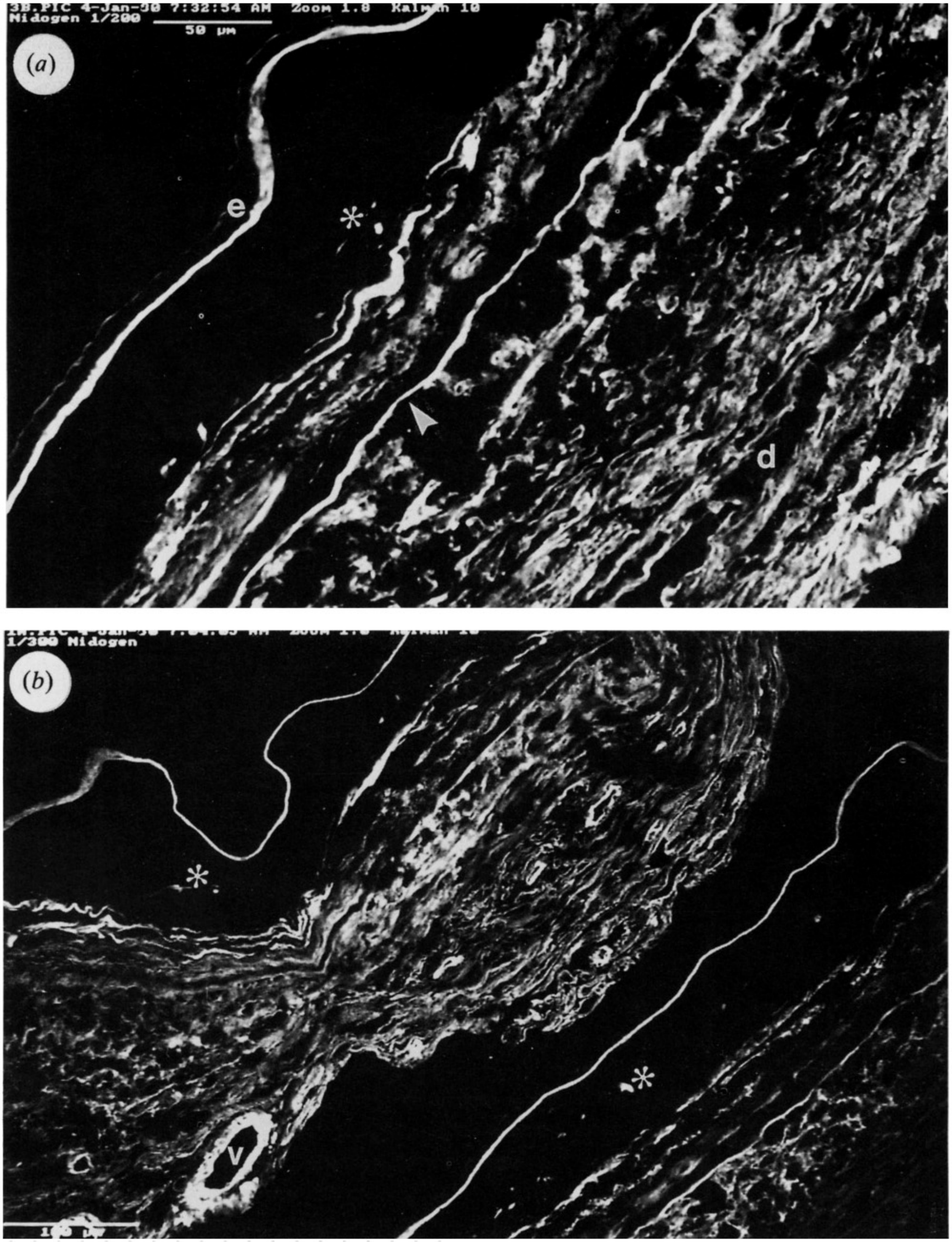

Figure 7. Confocal indirect immunofluorescence micrograph showing the distribution of anti-nidogen immunoreactivity. The immunoreactivity pattern is very similar to that of the type IV collagen and laminin. (*a*) There is strong fluorescence in the amniotic epithelial (e) and trophoblastic basement membrane (arrow) as well as in the decidua (d). The trabeculae in the fibroblast layer are strongly immunoreactive (asterisk). (*b*) Decidual blood vessels reveal intense specific immunofluorescence in vessel walls coincident with endothelial basement membranes (v). The trabeculae in the fibroblast layer are strongly immunoreactive (asterisk). Scale bar denotes (*a*) 50 µm, (*b*) 100 µm.

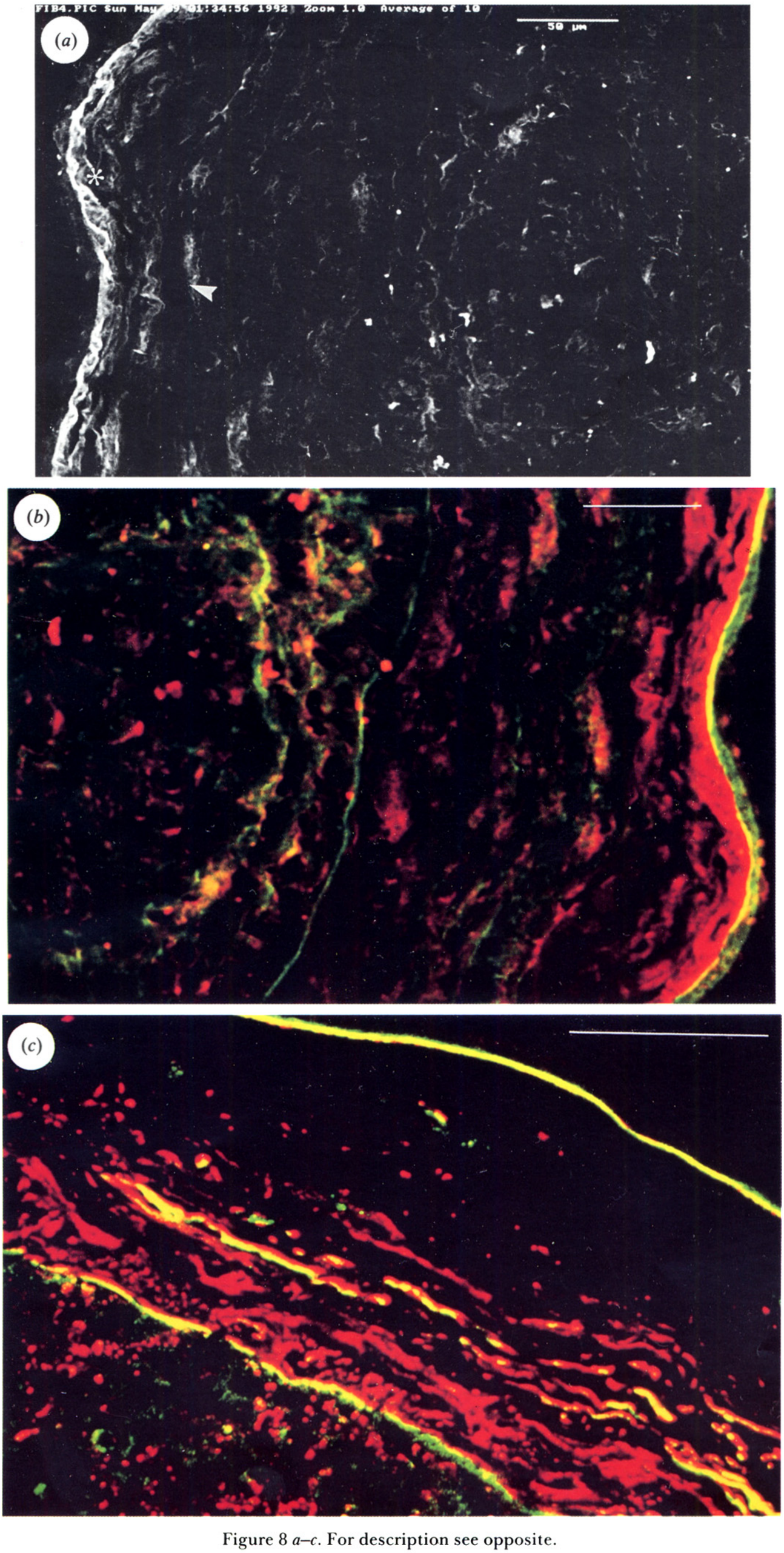

Figure 8 *a–c*. For description see opposite.

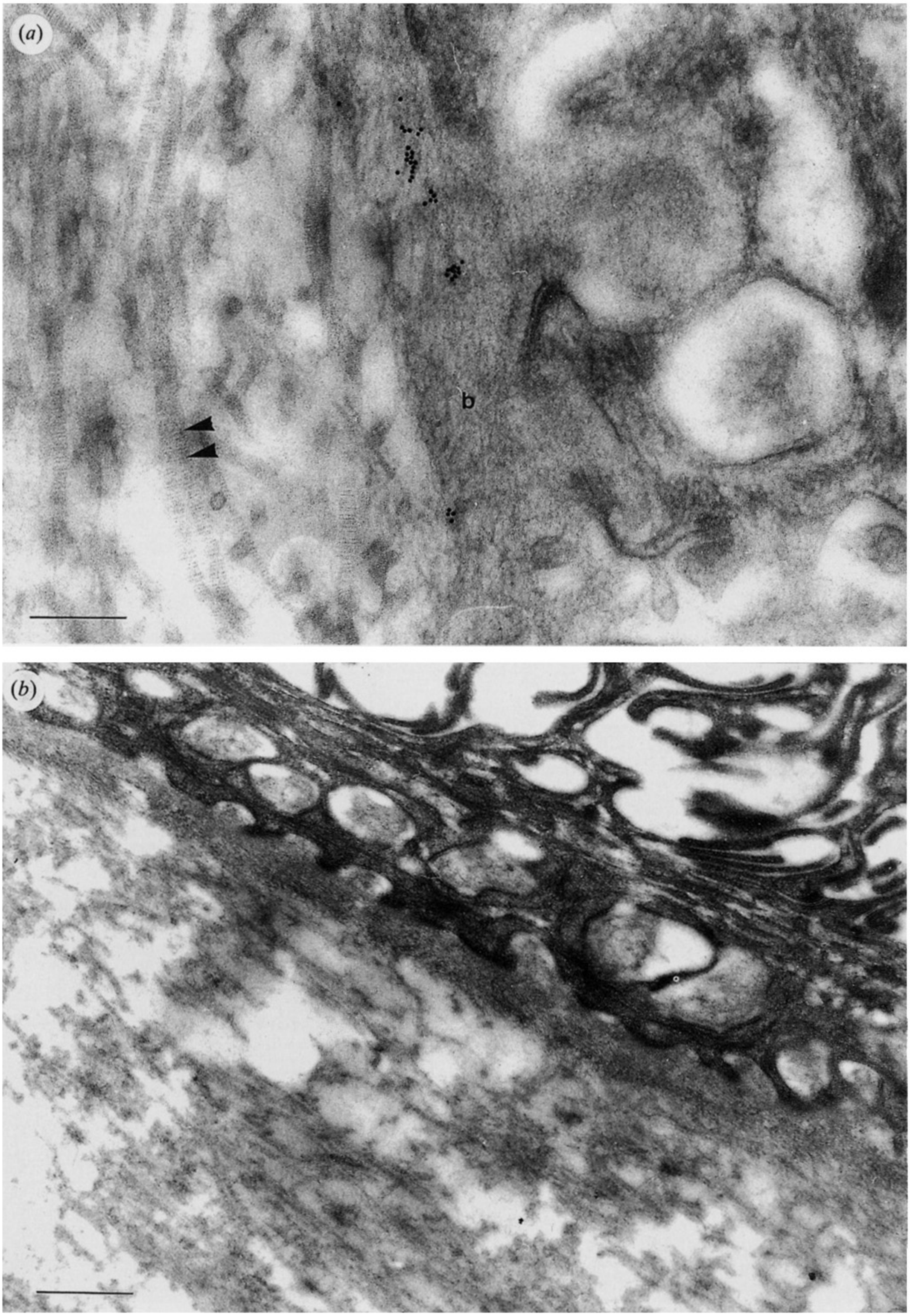

Figure 9. (*a*) Electron micrograph of low-temperature, low-denaturation embedded tissue. The electron dense colloidal gold particles reveal the sites immunoreactive with anti-IV collagen. In this field labelling is restricted to the amniotic epithelial basement membrane (b). Note the absence of label over the banded collagen fibres of the compact layer (arrows). (*b*) A similar field from a control preparation in which the sites were blocked with an excess of unlabelled antibody to show the background level of labelling. Scale bars denote (*a*) 0.2 μm, (*b*) 0.5 μm.

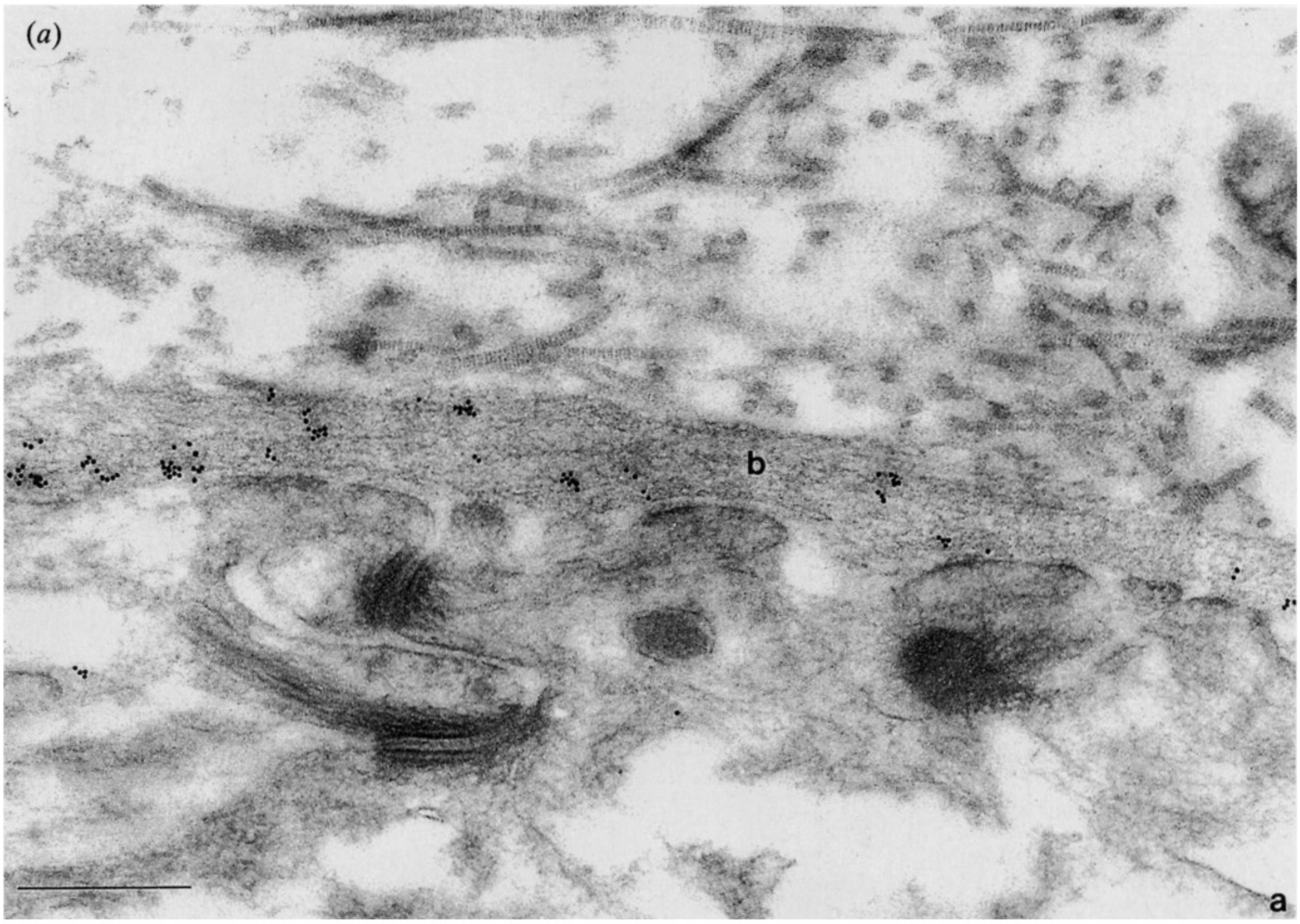

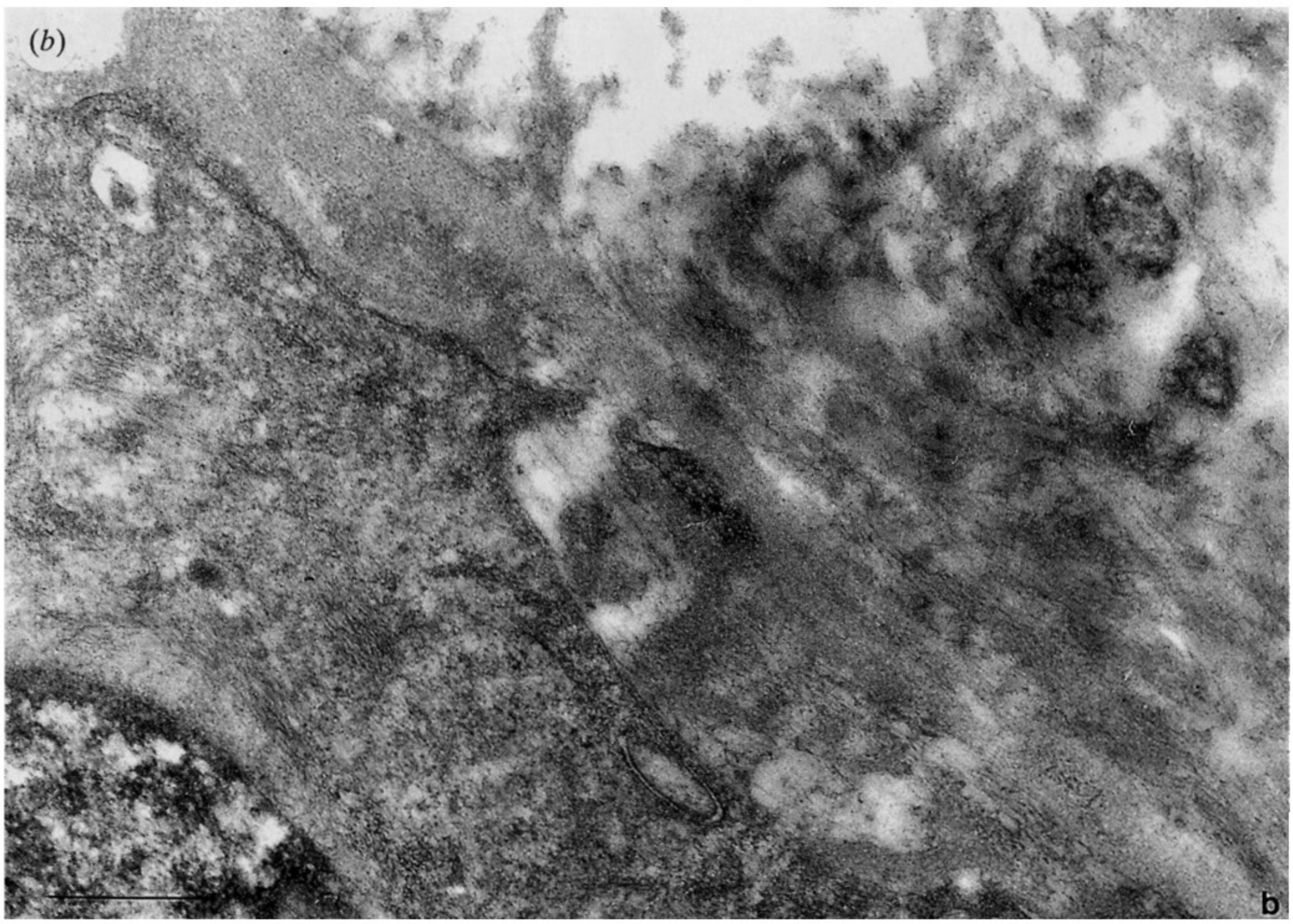

Figure 10. (*a*) Electron micrograph of low-temperature, low-denaturation embedded tissue. The electron dense colloidal gold particles reveal the sites immunoreactive with anti-type IV collagen. In this field labelling is restricted to the basement membrane (b) of the trophoblastic epithelium. (*b*) A similar field from a control preparation in which the immunoreactive sites were blocked with an excess of unlabelled antibody. Scale bars denote (*a*) 0.5 μm, (b) 0.5 μm.

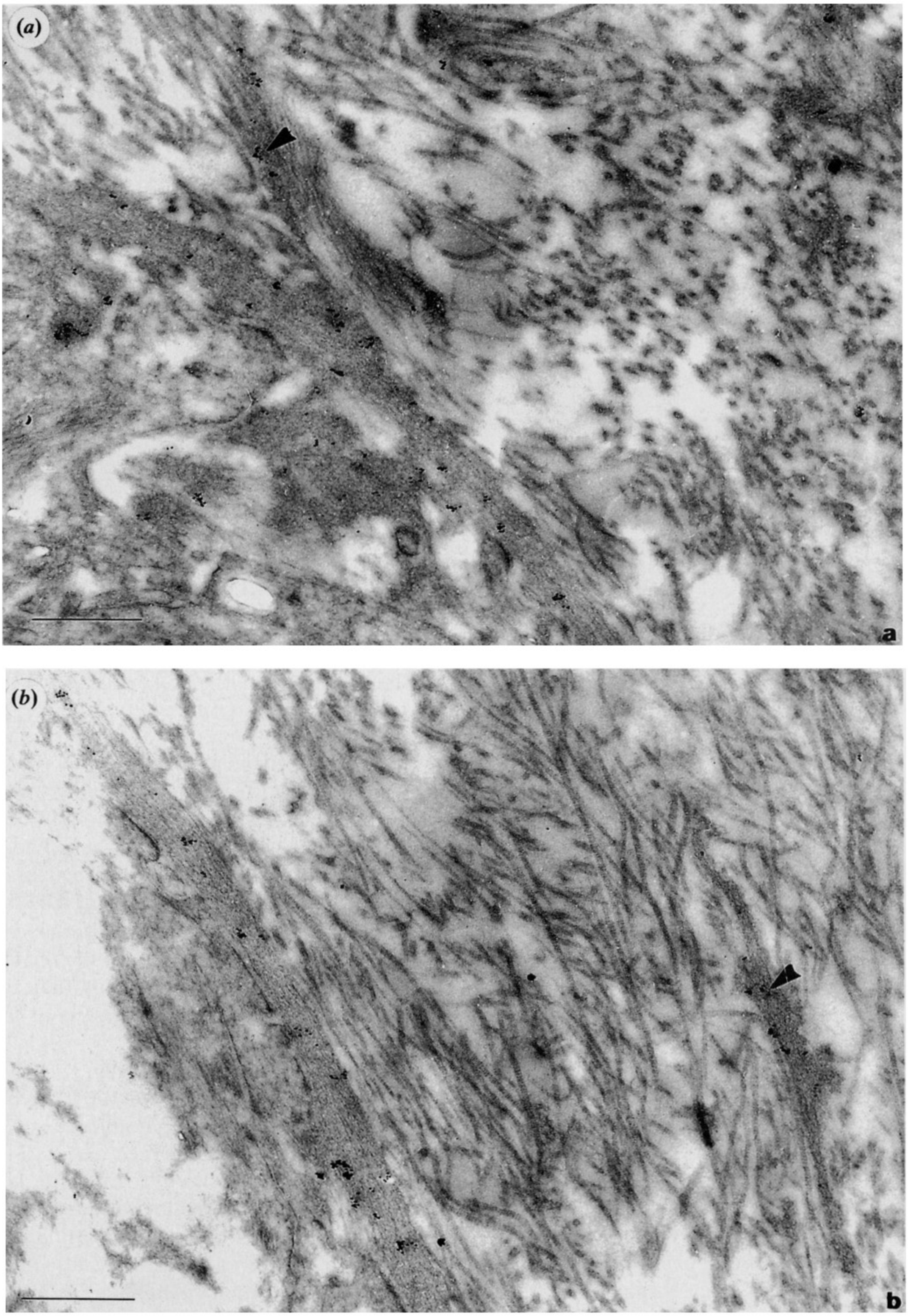

Figure 11. (*a*) Electron micrograph of low-temperature, low-denaturation embedded tissue taken from the site where the chorion laeve contacts the reticular layer. The electron dense colloidal gold particles reveal the sites immunoreactive with anti-type IV collagen. Note the strand of basement membrane-like material reaching out from the chorion laeve basement membrane into the neighbouring reticular layer connective tissue (arrow). Compare this with the structures seen at the light microscope level shown in figure 5 which also demonstrate anti-type IV collagen immunoreactivity. (b)Electron micrograph of low-temperature, low-denaturation embedded tissue taken from the site where the chorion laeve contacts the reticular layer. The electron dense colloidal gold particles reveal the sites immunoreactive with anti-type IV collagen. In this field labelling is restricted to the basement membrane and basement membrane-like material found in the reticular layer connective tissue (arrow). Scale bars denote (*a*) 0.5 μm, (*b*) 0.5 μm.

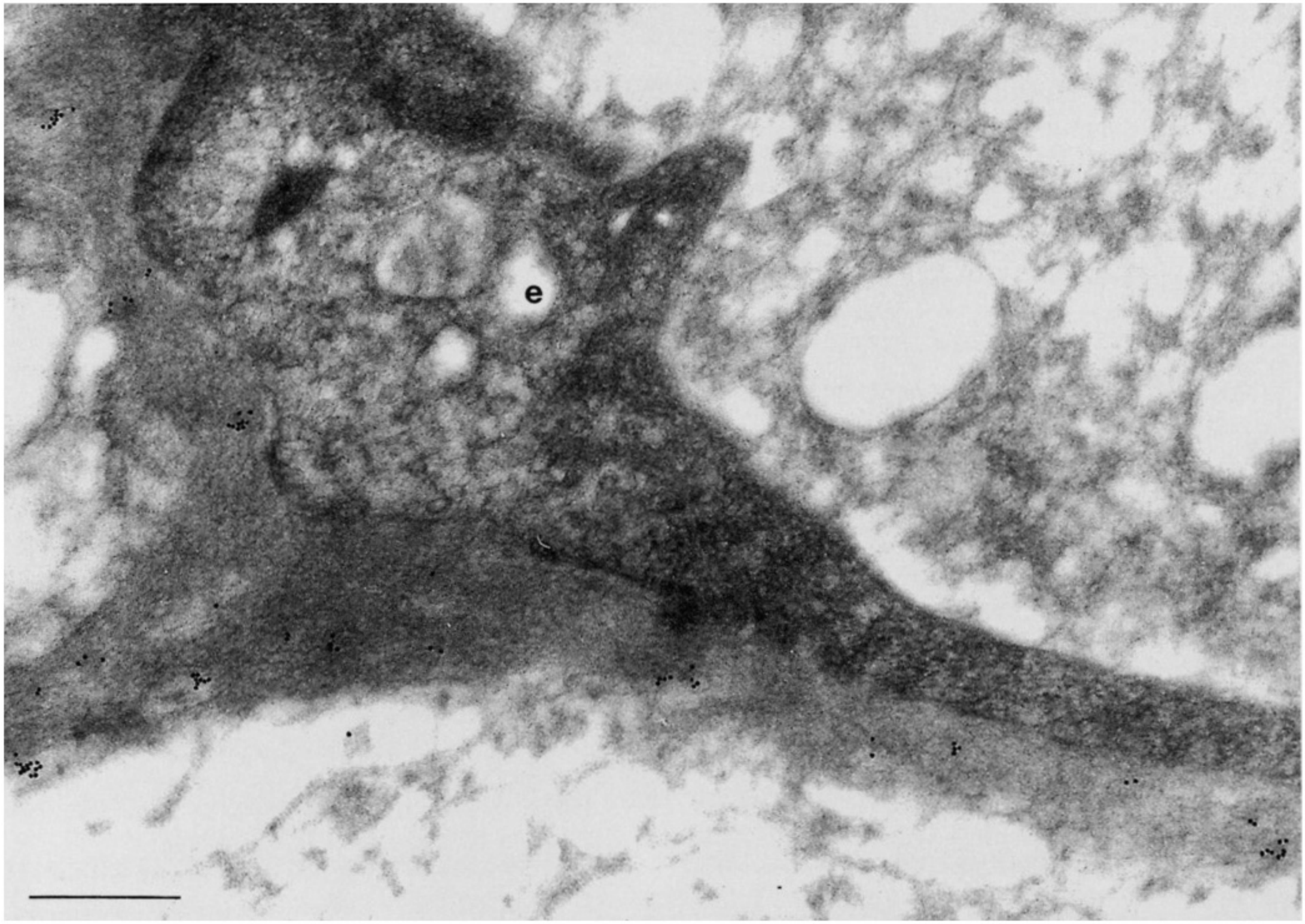

Figure 12. Electron micrograph of low-temperature, low-denaturation embedded tissue. The electron dense colloidal gold particles reveal the sites immunoreactive with anti-type IV collagen. In this field labelling is restricted to the endothelial basement membrane adjacent to a decidual capillary endothelial cell (e). Scale bar denotes 0.3 μm.